Article

Neutrophil Elastase-Activatable Prodrugs Based on an Alkoxyamine Platform to Deliver Alkyl Radicals Cytotoxic to Tumor Cells

Seda Seren,[||] Jean-Patrick Joly,[||] Pierre Voisin,* Véronique Bouchaud, Gérard Audran, Sylvain R. A. Marque, and Philippe Mellet*

Read Online

ACCESS | Metrics & More | Article Recommendations | Supporting Information

ABSTRACT: Current chemotherapies suffer low specificity and sometimes drug resistance. Neutrophil elastase activity in cancer is associated with poor prognosis and metastasis settlement. More generally, tumors harbor various and persistent protease activities unseen in healthy tissues. In an attempt to be more specific, we designed prodrugs that are activatable by neutrophil elastase. Upon activation, these alkoxyamine-based drugs release cytotoxic alkyl radicals that act randomly to prevent drug resistance. As a result, U87 glioblastoma cells displayed high level caspase 3/7 activation during the first hour of exposure in the presence of human neutrophil elastase and the prodrug in vitro. The apoptosis process and cell death occurred between 24 and 48 h after exposure with a half lethal concentration of 150 μM. These prodrugs are versatile and easy to synthetize and can be adapted to many enzymes.
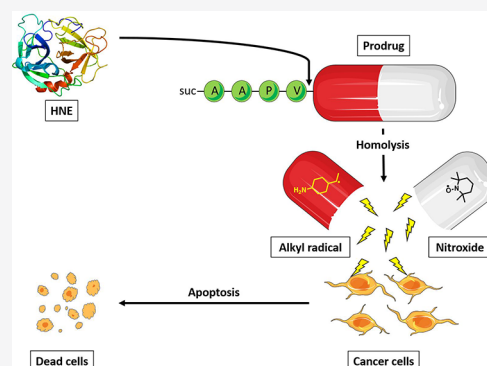
INTRODUCTION

Antimitotic chemotherapy drugs are currently used with some success as a standard treatment against cancer. They are however unable to therapeutically target a number of tumor types or their metastasis leading to millions of deaths worldwide. Several reasons have been identified. Since these drugs target dividing cells, their toxicity and low specificity prevent the use of the highest doses that would be necessary to reach the most resistant tumors and metastasis. Such toxicity also hinders the immune system, while it would be needed for tumor elimination. As importantly, some cancers acquire resistance to these drugs.

One way to circumvent the lack of specificity problem is to act through a prodrug step. The prodrug then needs to be activated in situ. In normal tissues, protease activity is strictly regulated by high concentrations of inhibitors, leading to very short times of activity. Consequently, this normal activity is hardly detectable. Interestingly, tumors and metastasis microenvironments display persistent protease activities [Matrix metalloproteinase (MMP), Urokinase, Plasmin, Cathepsin B, and prostate-specific antigen] that are not present in normal tissues.[1−3] Consecutive to this observation, inhibitors have been developed. Although positive results were sometimes observed, clinical trials were disappointing and rapidly abandoned. The main reasons were that proteolytic activities are redundant and that really selective inhibitors are difficult to design. Thus, the idea emerged to use these activities instead of inhibiting them. In recent years, attention has been drawn to the presence of neutrophil elastase (NE) activity in tumors and metastases. The origins and occurrence of this activity have been reviewed recently.[4,5] The presence of NE has been associated with a poor survival rate in

human breast cancer.[6] It is also suspected to take part in the etiology of other cancers.[7] Active NE appears essential to metastasis spreading and settling.[8−11] The origin of elastase activity in tumors is still debated. For instance, one team detected elastase in the supernatants of several human breast cancer cell lines in culture and in numerous tissue extracts prepared from human breast cancers.[12] Other works show that the active NE originates from tumor infiltrating granulocytic myeloid-derived suppressor cells, providing a pro-tumorigenic environment that can be partially suppressed by an elastase inhibitor.[13] Interestingly, patients with a lung cancer have significantly higher concentrations of elastase in their broncho-alveolar lavages than patients with chronic obstructive pulmonary disease although the latter carry a chronic lung inflammation.[14] Thus, NE activity may be a selective way to target tumors and metastasis at least in the absence of another inflammatory context.

In 2014, we suggested that alkoxyamines could be turned into prodrugs activated by proteases as a way to deliver cytotoxic alkyl radicals in the tumor microenvironment.[15] Thus, instead of trying to inhibit these activities, we proposed to use them to activate alkoxyamine prodrugs within the tumor environment. We later showed that activated alkoxyamines are indeed

cytotoxic through the activation of apoptosis. Toxicity is carried by the freshly generated alkyl radicals since high concentrations of a radical scavenger rescue the cells in culture.[16] Alkyl free radicals react with cells by creating random alterations. Thus, it would be more difficult for cancer cells to acquire a resistance to the drug. Alkoxyamines are metastable molecules that can be tuned to homolyze spontaneously at 37 °C. The homolysis generates a short-lived alkyl radical that is cytotoxic and a stable nitroxide that can be used to monitor the homolysis using Overhauser-enhanced magnetic resonance imaging.[16] It is also possible to graft a substrate at a key position to stabilize or activate.[17−19] To target proteases, a peptide can be grafted. By choosing the peptide, it is possible to target a specific protease (see Scheme 1). Thus, our approach relies on two concepts: a

Scheme 1. General Scheme for Elastase-Activated Alkoxyamines
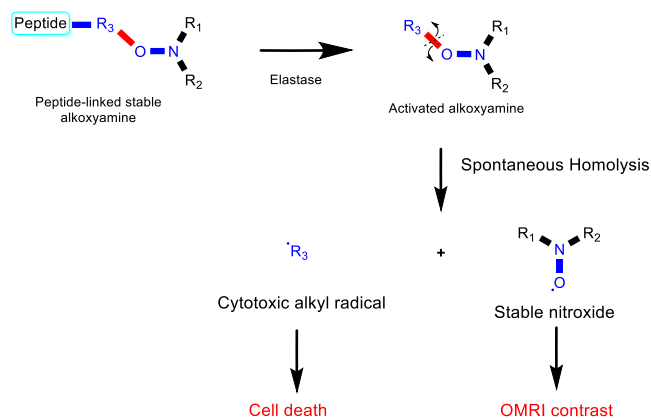
specific enzymatic activity and the spontaneous and instantaneous homolysis of free alkoxyamine to release cytotoxic free alkyl radicals.
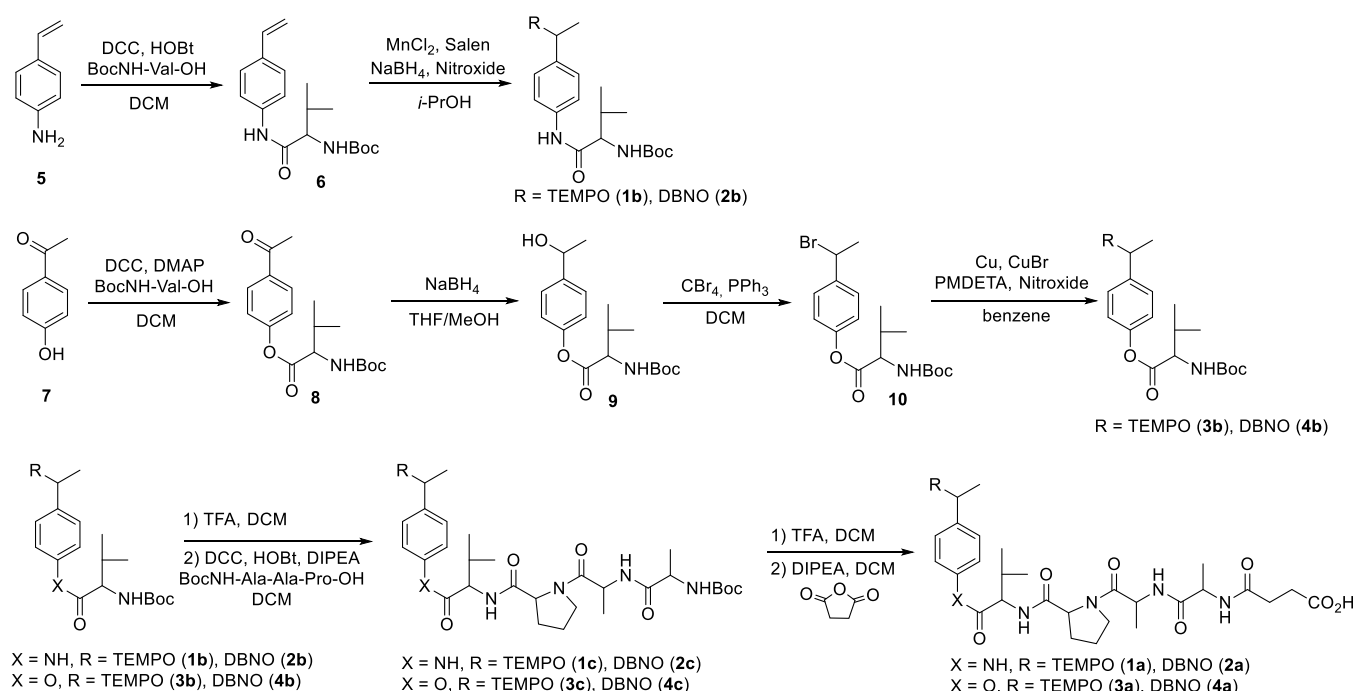
In this work, we designed and synthetized a series of alkoxyamines based on phenol or aniline cores stabilized with a peptide that is targeting NE. We review their enzymatic activation properties and their effect on cells in the presence or absence of enzymes, and we briefly study their mode of action.

RESULTS

Four molecules have been designed to be prodrugs that are activatable by NE to release free radicals. Two of them are based on a peptide-anilide coupled to either TEMPO or DBNO as for the nitroxide moiety. The two others differ only by being based on a peptide-phenoxy moiety.

Synthesis. For preparing **1a−4a**, two synthetic routes were used (see Scheme 2). For the first route, the peptide is attached to the alkoxyamine by an amide bond. For this, 4-vinylaniline was used to carry out peptide coupling with BocNH-Valine in order to obtain **6** in 78% yield. Then to introduce the nitroxides, TEMPO and DBNO, coupling with manganese and with the Salen ligand[20] was carried out to obtain the two alkoxyamines **1b** and **2b** in 65 and 57% yields, respectively. For the second route, the peptide is attached to the alkoxyamine by an ester bond. A Steglich esterification[21] was carried out between 4-hydroxyacetophenone and BocNH-Valine to afford **8** quantitatively. The ketone was then reduced to alcohol with NaBH$_4$, and then this alcohol was substituted with bromine using the Appel reaction[22] affording **10** in 53% yield over both steps. The TEMPO and DBNO nitroxides were then introduced by an A.T.R.A. coupling[23] to yield alkoxyamines **3b** (86%) and **4b** (93%).

To finalize the synthesis, the peptide addition was completed on alkoxyamines **1b−4b**. The Boc group was cleaved using trifluoroacetic acid (TFA), and then the peptide coupling step was carried out to introduce the continuation of the peptide (NHBoc-Ala-Ala-Pro-OH) to obtain the alkoxyamine **1c−4c** in yields from 51 to 73%. The last step is the deprotection of the Boc group by TFA followed by the addition of the succinyl

Scheme 2. Synthesis of the Prodrugs 1a to 4a

Scheme 3. Expected Reaction Paths of the Prodrugs in the Presence of HNE
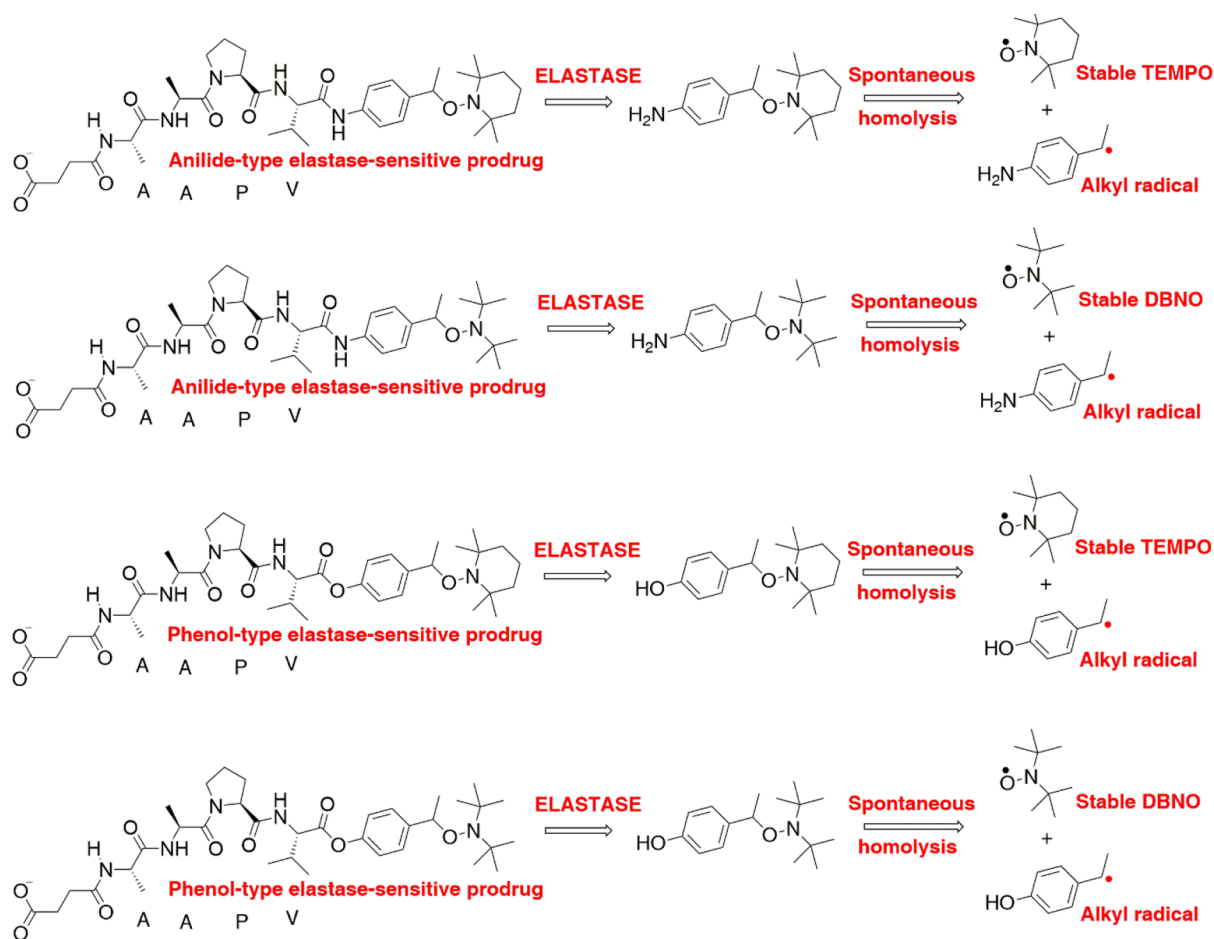
group with succinic anhydride to afford **1a–4a** in 76 to 86% yields.

All the Prodrugs are Specifically Activated by NE. All four prodrugs have been designed so that the stabilizing peptide can be hydrolyzed by human neutrophil elastase (HNE). Then the activated prodrugs should homolyze to two free radicals: a very unstable alkyl radical and a stable nitroxide (Scheme 3).

Suc-AAPV peptide has been used to model many chromogenic or fluorescent substrates for NE. This peptide spans the S1 to S4 sites of the enzyme. All alkoxyamines based on this peptide were readily hydrolyzed by the targeted enzyme generating an activated alkoxyamine. As an example, in Figure 1, high-performance liquid chromatography (HPLC) traces show that the free peptide is released as expected from the suc-AAPV-Anilide-TEMPO alkoxyamine in the presence of the enzyme.

Alkoxyamine activation results in homolysis generating two free radicals: a transient alkyl radical and a stable nitroxide. Thus, monitoring the kinetics of generation of the nitroxides TEMPO and DBNO by electron paramagnetic resonance (EPR) is a safe method to monitor the enzymatic activation. Figure 2 shows that all prodrugs are activated in the presence of HNE. The anilide-TEMPO model has the best prodrug properties since no TEMPO release was detected in 16 h at 37 °C in the absence of enzyme. The other models, however, are leaking TEMPO or DBNO which could cause interpretation problems in the cytotoxicity tests and toxicity in future in vivo applications. Two mechanisms are identified for this leakage: (1) spontaneous hydrolysis of the peptide-phenol bond, which is weaker than the

peptide-anilide bond and (2) spontaneous homolysis of the DBNO alkoxyamine model, which is intrinsically more labile than TEMPO-derivatives. In the phenol-DBNO model, both mechanisms are cumulatively yielding the less stable prodrug.

In Figure 2, apparent rates of homolysis in pure buffered solution are low. This slow reaction is due to an equilibrium between the free radicals and the reformed alkoxyamine. This reaction eventually ends by the combination of the two alkyl radicals, which is not reversible. This so-called "persistent radical effect" has been fully described.[24] This is not predictive of the kinetics in a biological medium that contains many types of radical scavengers. Indeed, addition of galvinoxyl reveals much faster homolysis (Figure 3) with a rate nearly 400 times higher. This means that in the presence of reactive groups, the alkyl radical is readily available to alter cellular components. The same kinetics acceleration can be obtained with the nitroxide SG-1 (not shown).

The specificity of the chosen peptide suc-AAPV-for elastase was confirmed as we did not observe any TEMPO release with trypsin, urokinase and chymotrypsin (not shown).

Three Out of the Four Prodrugs are Cytotoxic on the Human Glioblastoma U87 Cell Line In Vitro in the Presence of HNE Only. Figure 4A displays the viability of U87 cells 48 h after exposure to the four alkoxyamines in the presence or absence of HNE. HNE itself did not have any effect on viability. Within the range of 0–400 μM and in the absence of HNE, the prodrugs have no measurable effect except for suc-AAPV-phenol-TEMPO at 400 μM. The addition of HNE
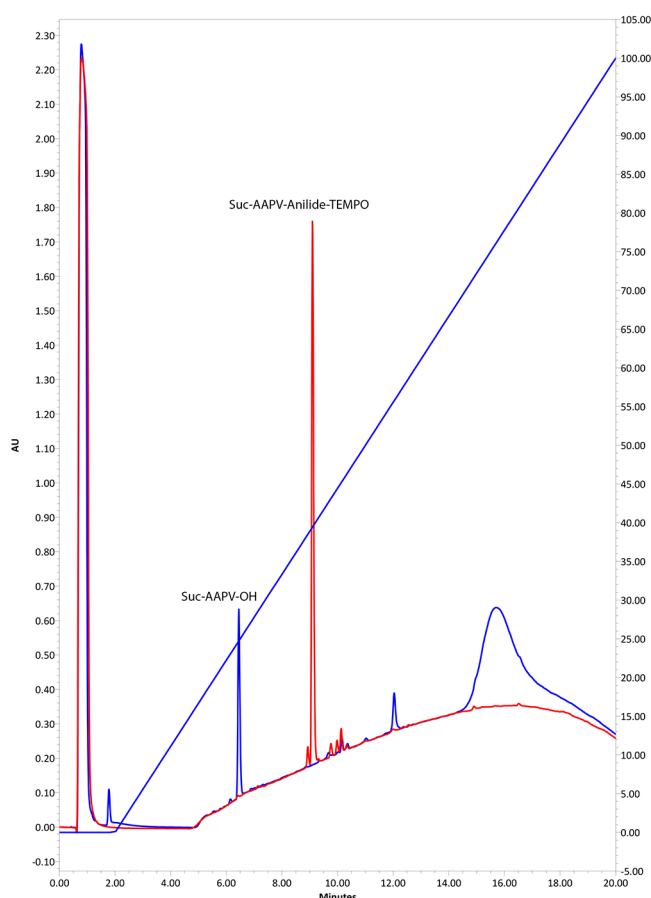
Figure 1. HPLC traces showing purity of the native alkoxyamine (red trace) and the release of the free peptide in the presence of HNE (blue trace).

reveals a dose-dependent effect on viability except for suc-AAPV-Phenol-DBNO that does not have any measurable effect despite its activation by HNE. In our experimental setup, the LC50 was obtained around 150 μM for suc-AAPV-anilide-TEMPO, suc-AAPV-anilide-DBNO, and suc-AAPV-Phenol-TEMPO. The viability also has been probed versus the time with the suc-AAPV-anilide-TEMPO model (Figure 4B). Cytotoxicity in the presence of HNE is already pronounced at 24 h and marginally evolves at 48 and 72 h. At 72 h, the difference with 48 h is detectable only for the lowest doses. In the absence of HNE, cell viability is kept at 100% at all times and concentrations, making suc-AAPV-anilide-TEMPO a safe prodrug.

Presence of Active HNE is Required for Cytotoxicity. Dose response experiments were reproduced on the four prodrugs except that eglin C, a potent HNE inhibitor, was added just before HNE in the cultures. Figure 5 shows that adding eglin C rescues the cells in all experiments. Thus elastase activity is required to kill the U87 cells.

Freshly Generated Alkyl Radicals are the Origin of the Cytotoxic Effect of the Activated Drug. The prodrugs were designed to kill cells through the in situ generation of cytotoxic alkyl radicals. To assess this mechanism, we needed to check that the effect was due to unstable alkyl free radicals and not to secondary chemicals like toxic anilines or toxic phenols. For this purpose, two types of experiments were conducted. In the first experiment, solutions of suc-AAPV-anilide-TEMPO or suc-AAPV-phenol-TEMPO were mixed with HNE in DMEM and left 24 h at 37 °C to reach the exhaustion of the chemical reactions. These solutions were then applied to the cell culture for 48 h in the same conditions as for the abovementioned cytotoxicity tests. Figure 6 clearly shows that exhausted solutions that are deprived of the reactive alkyl free radicals are not toxic for the U87 cells.
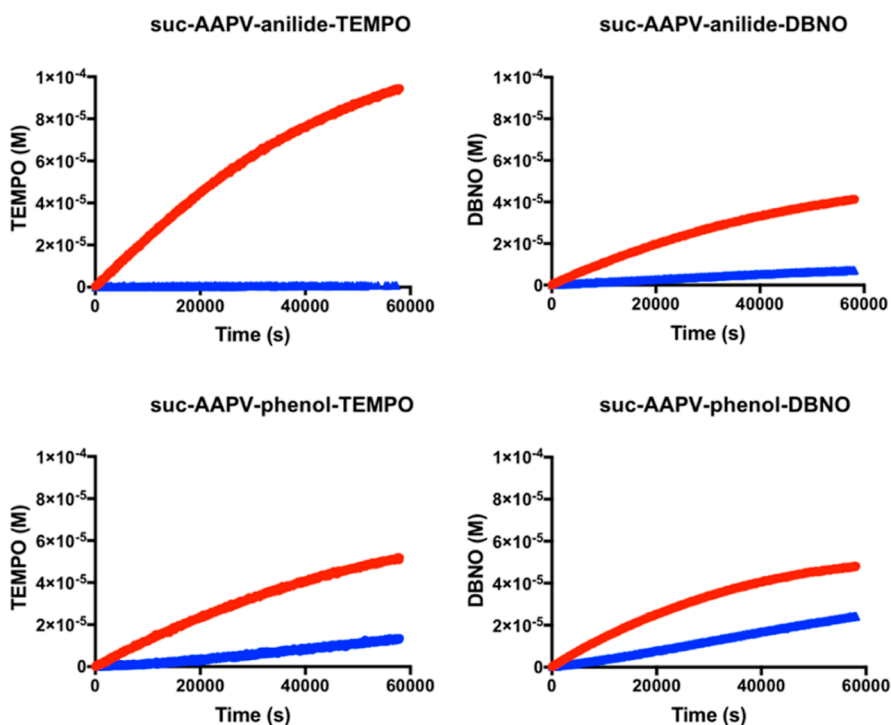

Figure 2. Monitoring of the release of TEMPO and DBNO by EPR in the presence (red curves) or absence (blue curves) of HNE (20 nM) at 37 °C assessing the enzymatic activation and the subsequent homolysis of the alkoxyamines.
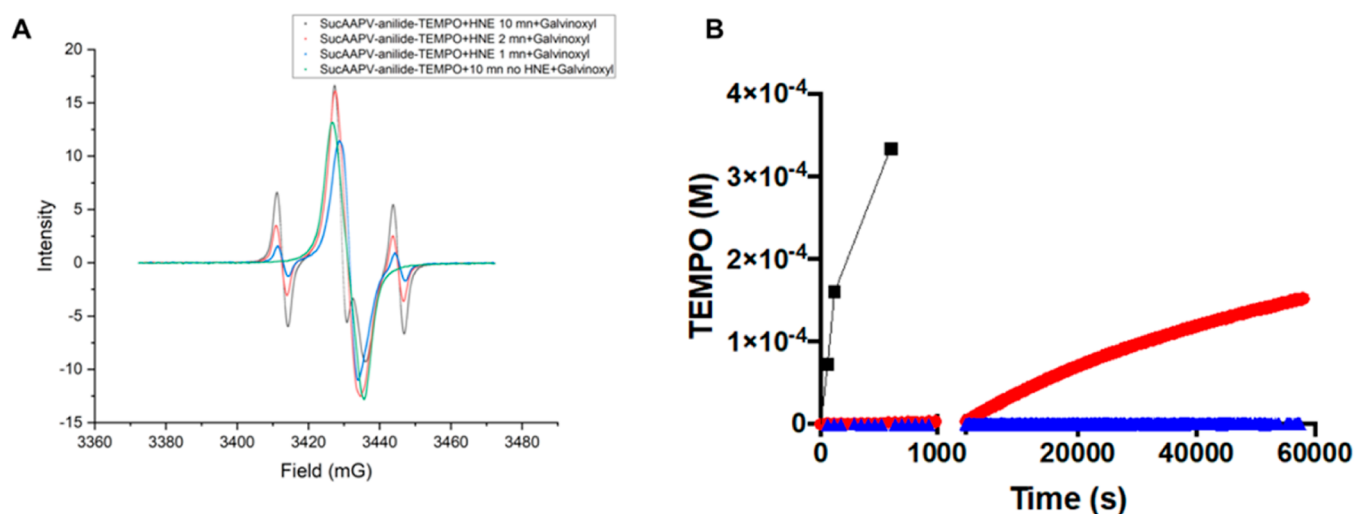
Figure 3. Acceleration of TEMPO release in the presence of a free radical scavenger: (A) EPR spectra of a solution of suc-AAPV-anilide-TEMPO with or without HNE (1.6 μM). The enzymatic reaction was stopped by adding galvinoxyl in THF 1/1 at 1 min (blue line), 2 min (red line) and 10 min (black line) incubation at 37 °C. A control stopped at 10 min incubation without HNE is shown in green. In this control, only galvinoxyl is detected. (B) Plot of the released TEMPO versus time in the presence of galvinoxyl (black line) compared to the kinetics without galvinoxyl (red line with HNE (0.68 μM), blue line without HNE).

In the second series of experiments, suc-AAPV-anilide-TEMPO and suc-AAPV-phenol-TEMPO cytotoxicity in the presence or absence of HNE were probed at increasing concentrations of troxerutin, a free radical scavenger that is not toxic for cell culture. Figure 7A,B shows that increasing concentration of troxerutin leads to increasing protection of the cells reaching complete protection at 150 mM.

Thus, the prodrugs' cytotoxicity only occurs by freshly generated free radicals and is cancelled by a free radical scavenger. This comforts our postulate that in situ generation of very reactive alkyl radicals is a promising way to kill cancer cells.

Cell Death Occurs following Caspase 3/7 Activation and Apoptosis. U87 cells were treated with the alkoxyamine suc-AAPV-anilide-TEMPO at three different concentrations that generate 25, 50, and 90% loss of viability 48 h after contact. The development of a potential apoptosis/necrosis status was observed at 1, 3, 7, 24, and 48 h after contact with the alkoxyamine looking at the caspase 3/7 activation (casp+) (Figure 8), the phosphatidylserine translocation (annexin V labeling, AV+), and the cell membrane loss of integrity (DNA staining, DNA+). Caspase 3/7 activation would discriminate the development of a necrosis status (casp−) from the apoptotic one (casp+). Annexin V and DNA staining allow the characterization of the early apoptotic cells (AV+, DNA−) and the late apoptotic/necrotic cells (AV+, DNA+).

Between 1 and 48 h, the presence of either HNE alone or the alkoxyamine alone did not induce neither the caspase 3/7 activation nor the phosphatidylserine translocation nor cell membrane permeability to the DNA marker. This is in accordance with the viability study showing 100% viability after 48 h exposure. In contrast, the alkoxyamine in the presence of HNE triggers a rapid and complete apoptotic process.

For 150 and 250 μM concentrations that generate 50 and 90% lethality, respectively, the caspases 3/7 appear strongly activated as soon as 1 h after exposure. They keep a high level activity until 7 h and then decrease. For alkoxyamine at 75 μM, the caspase 3/7 activity appear noticeably above the basal level but lower than for the other concentrations. The same pattern is also apparent for annexin V and DNA labeling, probably reflecting a lower

number of cells engaged in apoptosis. For the highest alkoxyamine concentrations, the annexin V labeling increases its level until 7 h like for the caspase 3/7 activity. Then these apoptotic cues decrease until 48 h. Simultaneously, the DNA labeling for all the tested alkoxyamine increases with time reaching its maximal level between 24 and 48 h. So, these observations reveal an evolution of the apoptosis/necrosis processes that is rapidly engaged after 1 h of exposure. It ends with necrosis affecting the alkoxyamine sensitive cells at 24/48 h.

For apoptosis test control, U87 cells were also treated with doxorubicin 2 μM known to be a DNA double strand linker. Concentration was adjusted to get 50% of the U87 population still viable after 48 h for a convenient comparison with alkoxyamines. The timing of the apoptosis/necrosis development is strongly delayed when compared to the alkoxyamine 150 μM treatment that affects also 50% of the cell population. The caspase activity increases between 24 and 48 h. The cells are highly AV+ following a similar timing, whereas the DNA+ labeling increases regularly until 48 h.

This different profile suggests that the prodrug alkoxyamine in the presence of HNE activation triggers other pathways that induce very early apoptosis/necrosis.

■ DISCUSSION

The aim of this work was to design to prepare and to test prototypes of a prodrug that releases cytotoxic-free radicals upon activation by a specific protease. The secondary aims were to design a prodrug without any cytotoxicity before activation and with a size that is compatible with renal elimination to avoid any undesired toxic accumulation. By design, we also aimed at making drug resistance unlikely since cytotoxic alkyl radicals act randomly on cell components.

High yield synthesis succeeded with six steps for the anilide-based alkoxyamines and eight steps for the phenol-based alkoxyamines. This predicts low cost for the eventual production of the prodrug. Kinetics studies show that it is possible to make a prodrug activatable by HNE that delivers a cytotoxic alkyl radical and a stable nitroxide. All data converge toward the choice of the suc-AAPV-anilide-TEMPO model: in the absence
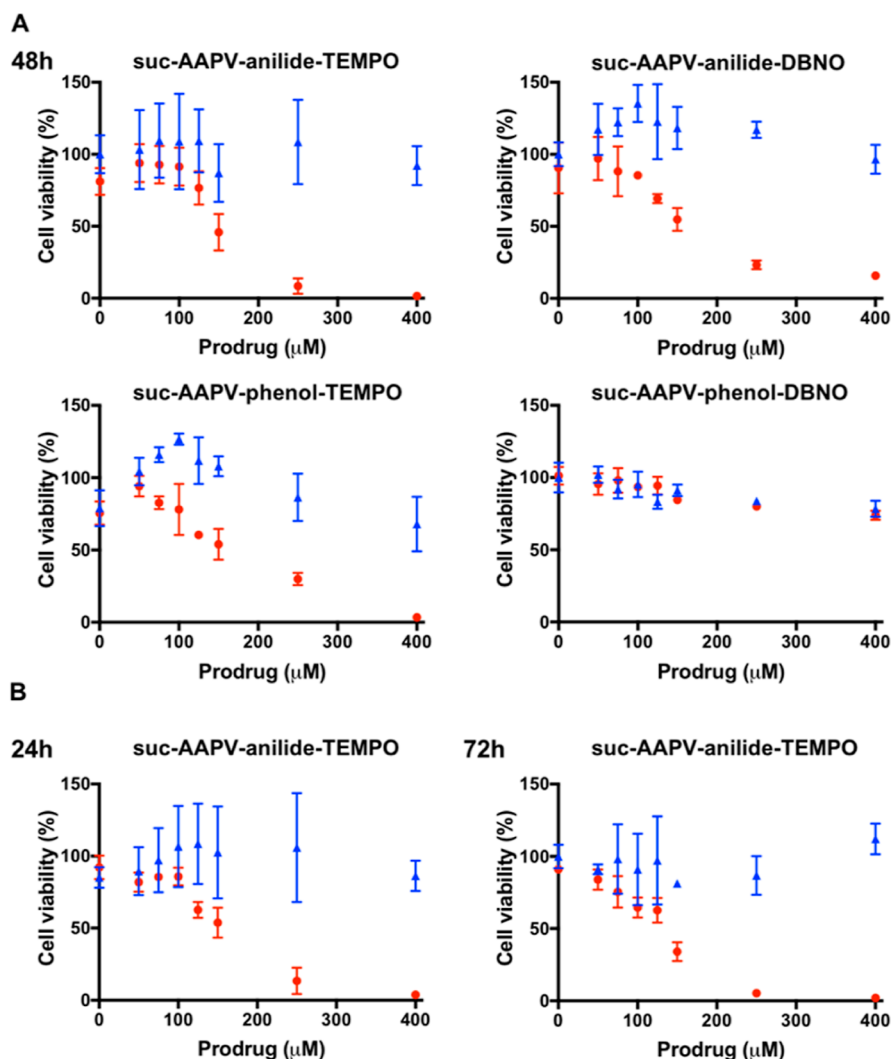
Figure 4. Viability of U87 cells in the presence of the prodrugs ± HNE. (A) Dose response study of the viability of U87 cells against suc-AAPV-anilide-TEMPO, suc-AAPV-anilide-DBNO, suc-AAPV-phenol-TEMPO, and suc-AAPV-phenol-DBNO in the presence (red symbols) or absence (blue symbols) of added HNE (0.68 μM). (B) Dose response study of the viability of U87 cells against suc-AAPV-anilide-TEMPO at 24 and 72 h in the presence (red symbols) or absence (blue symbols) of HNE (0.68 μM).

of HNE, EPR showed that it was stable at 37 °C for at least 16 h in biological buffer which is in agreement with the estimated activation energy of 130 kJ/mol. Accordingly, none of the markers linked to apoptosis was detectable, suggesting a safe elimination of the unreacted prodrug and thus a safe in vivo administration. However, its activation in the presence of HNE resulted in fast apoptosis triggering and cell death in a dose-dependent manner. This implies rapid activation by the enzyme and rapid homolysis of the activated alkoxyamine in the culture medium. Rapid phosphatidylserine exposition may be an advantage in vivo since it could trigger a so-called bystander effect through macrophage activation that would amplify tumor cell death.[25]

The cytotoxic effect goes through freshly generated alkyl radicals. This consolidates the idea of safer use since their lifetime is very short precluding diffusion and harm to nearby tissues. Overall, these properties suggest a potentially larger therapeutic range in comparison to previous prodrugs using very toxic components like anthrax toxin or doxorubicin that become more cell permeable or more bioavailable upon protease activation.[2,26] The cytotoxicity half effect comes at 150 μM.

This may seem elevated; however, it is tempered by the absence of cytotoxicity observed by viability count or apoptosis markers until at least 400 μM. Furthermore, alterations due to the alkyl free radical are probably cumulative, thus opening the possibility of replacing high concentration with a longer contact time, for instance, using low concentration intravenous infusion. It could also be a bias due to the test in 96-well plates. Indeed in these conditions, cells adhere to the bottom of the plate but the activation of the drug takes place in the whole volume of culture medium. Considering that the half-life of the alkyl radical in solution is well under a microsecond, it can diffuse only 30 nm before reaction. Thus most of the medium volume containing the enzyme activates the alkoxyamine with little chance to reach the adherent cells. If so, much less alkoxyamine may be needed in vivo since the activation should take place in the interstitial fluid, where the enzyme activities are, inside the tumor, a thin space very close to the cells. Also the cytotoxicity yield can very probably be enhanced by modifying the alkyl radical moiety for a better cell permeability. This is a real possibility due to the modular construction of the prodrug with the consequence that some sites of the molecule can be modified without altering the
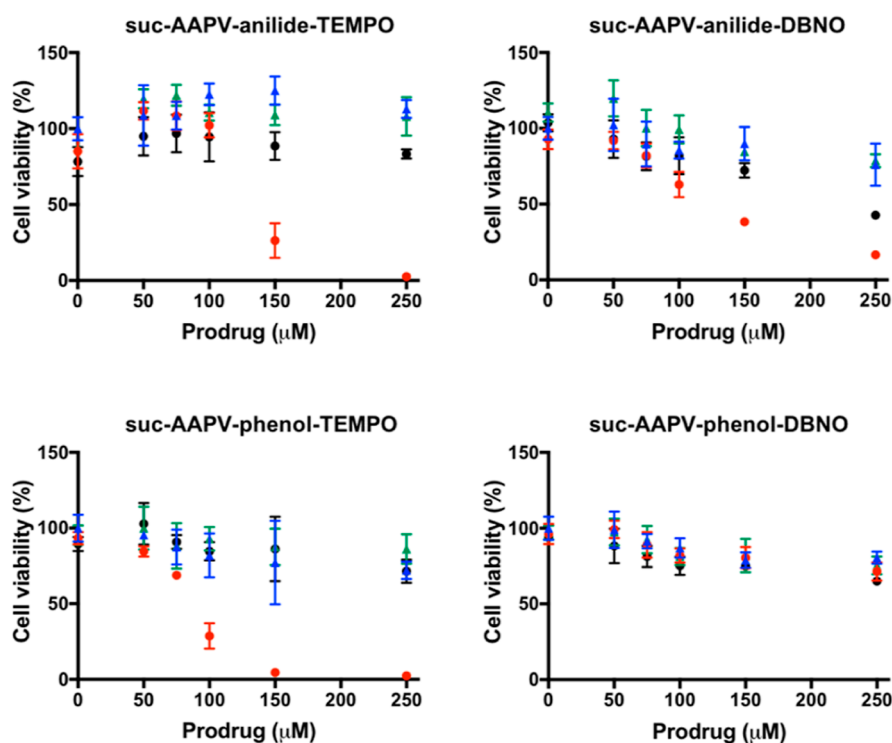
Figure 5. Effect of the elastase inhibitor eglin C on U87 cells rescue at 48 h. Conditions are identical to those in Figure 4 (prodrug only: blue symbols; prodrug in the presence of HNE (0.68 μM): red symbol) except for the addition of eglin C (10 μM) (prodrug in the presence of eglin C: green symbols; prodrug in the presence of eglin C and HNE (0.68 μM): black symbols).
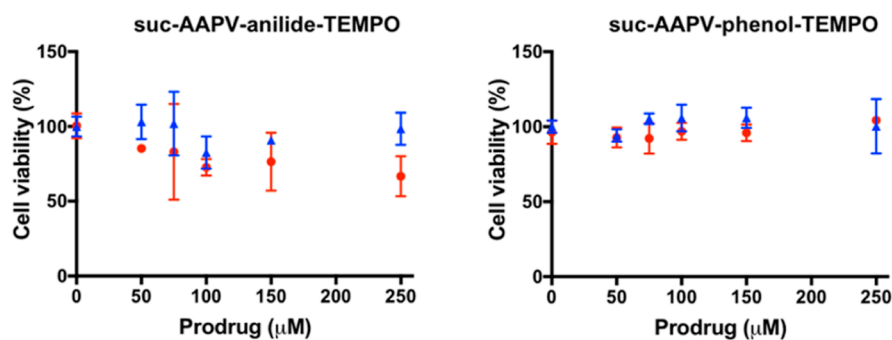

Figure 6. Viability of U87 cells after 48 h in the presence of suc-AAPV-anilide-TEMPO or suc-AAPV-phenol-TEMPO that were beforehand incubated 24 h with or without HNE (0.68 μM) to test the effect of free radicals exhaustion(red symbols with HNE; blue symbols without HNE).

physical chemistry of the homolysis nor the interaction with the enzyme.

For this "proof of concept" paper, HNE was added in the cell culture medium deprived of serum, left for an hour and inhibited by adding fresh serum. This protocol was chosen because U87 cells as many cancer cell lines in culture secrete only inactive pro-proteases. In tumors, these proteases are activated in cascade and a large part of the proteolytic activity is also provided by infiltrated non-tumor cells or surrounding fibroblasts.

HNE as a serine-protease with broad spectrum specificity is involved in matrix remodeling in a variety of pathological processes, namely, emphysema, chronic obstructive pulmonary disease, cystic fibrosis, atherosclerosis, and cancer.[4,27−30] HNE is primarily stored in azurophilic granules of neutrophils and released into the extracellular space through degranulation. HNE is also secreted by a variety of other immune cells, namely, MDSCs, macrophages, and lymphocytes.[31,32] As a matter of fact, HNE is upregulated in numerous cancer types. The HNE levels

appear significantly elevated in the setting of cancer, even when compared to non-malignant inflammatory diseases with the exception of cystic fibrosis. This situation has been described in the case of lung cancer or colon adenocarcinoma.[14,33,34] As described in prostate cancer, myeloid cells exert pro-tumorigenic actions through intratumoral HNE secretion and NET formation in response to cell signaling within the tumor microenvironment.[13] Nevertheless, studies on epithelial breast cancer cells suggest that a tumor cell origin of HNE is also possible.[12] Thus, HNE is considered as a tumorigenic contributor in numerous types of cancer and is considered as an independent prognostic indicator in patients with cancers of breast, lung, prostate, and colon.[4,6,30] HNE appears to act at the picomole level of active enzyme to induce angiogenesis and enhance the intravasation of tumor cells into a distinct set of dilated intratumoral angiogenic vessels.[8] Likewise, NE enables the vascular arrested tumor cells to resist clearance and survival in secondary tissue sites. Elastase-rich NETs could facilitate the
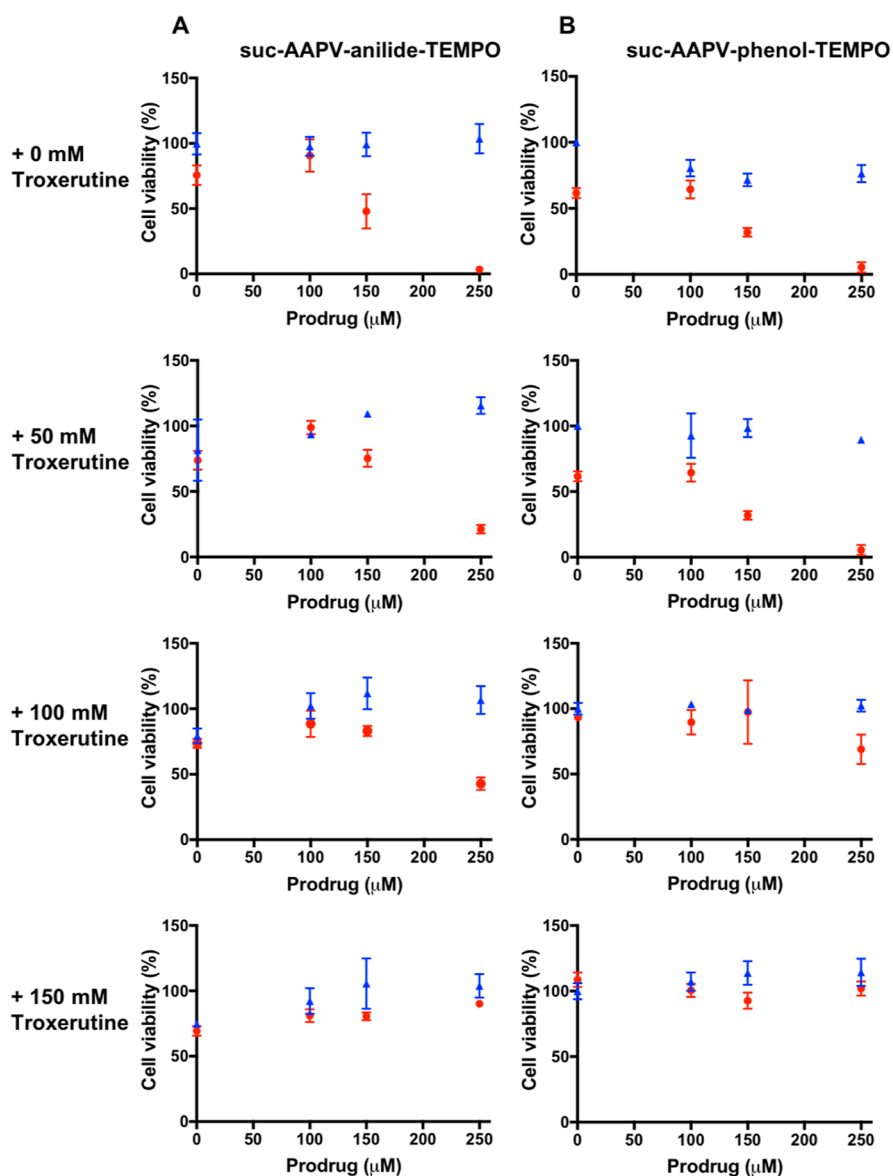
Figure 7. Rescue of U87 cells viability at 48 h by increasing addition of troxerutin (0, 50, 100, and 150 mM), a free radical scavenger. Cells were treated with (A) suc-AAPV-anilide-TEMPO or (B) suc-AAPV-phenol-TEMPO with (red symbols) or without HNE (0.68 μM) (blue symbols).

metastatic spread though the induction of the epithelial–mesenchymal transition. So, NE acts also at the limit between tumor cells and the vasculature avoiding the tumor cell clearance inside the blood circulation. Moreover the involvement of NE in tumorigenesis is strongly suggested since the NE genetic deletion (Elane −/−)[35] or the pharmacological inhibition reduces the tumor charge in some preclinical studies of cancer and leukemia.[4] Indeed using lung adenocarcinoma model mice lacking NE (Elane −/−), the NE contribution appears more in the tumor growth rather than initiation. However in other cases, NE is involved in tumor initiation in inflammation-induced cancers.[36] These observations are corroborated by the impact of NE inhibitors. NE inhibition by curcumin reduced Lewis lung carcinoma tumors in syngenic and xenograft mouse models.[37,38] Similarly, Sivelestat (ONO-5046) decreased tumor progression in mice bearing human colorectal, lung, gastric, prostate cancer xenografts,[13,39−41] thereby reproducing effects of antibody-mediated neutrophil depletion in xenotransplantation.

However, the experience of MMP inhibition strategies during the past decades showing limited efficiency in clinical trials suggests that the inhibition strategy is not sufficient. Hence, our approach is to utilize the existing enzyme activities instead of inhibiting the enzymes.

Considering the abovementioned facts, we chose to design the first prodrugs such that they are activated by NE. Interestingly, their structure is similar to the popular *para*-nitroanilide chromogenic substrates commonly used to detect and measure serine and cysteine protease activities simply by varying the peptide since the main substrate selection is done at the P1 position according to the Schechter and Berger nomenclature.[42] Similarly, our prodrugs may be able to target more serine and cysteine proteases that are described in the tumor microenvironment, that is, the serine protease urokinase, fibroblast activation protein,[43,44] or prostate specific antigen, and the cysteine proteases cathepsin B[2] or cathepsin V.[45] This was confirmed by all our molecular docking calculations (not shown). MMP activities are also important targets.[2] Since their
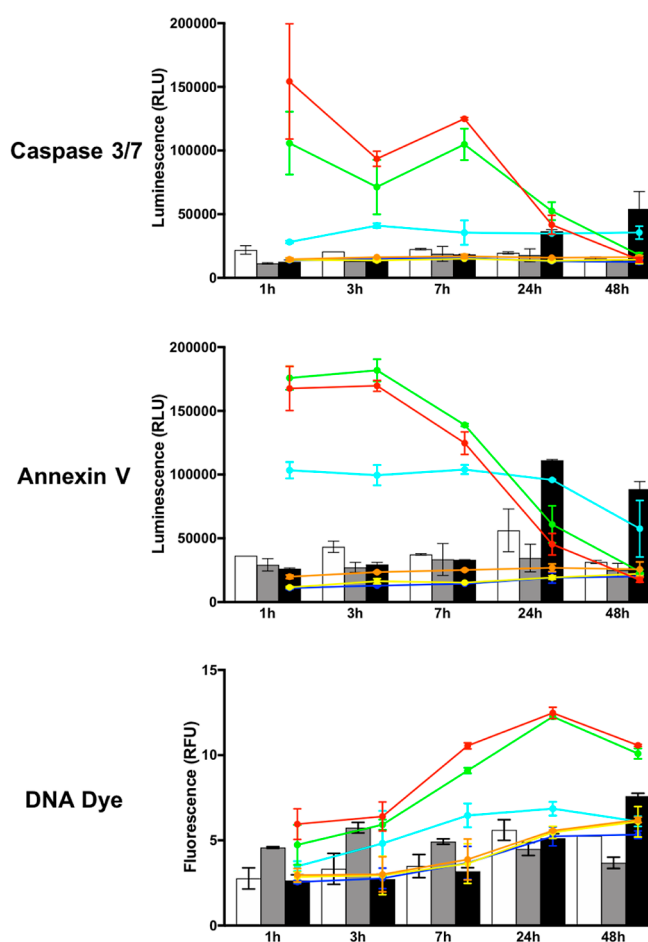
Figure 8. Timeline of cell death mechanisms with suc-AAPV-anilide-TEMPO. Cells were treated with 75 μM (cyan line), 150 μM (green line), and 250 μM (red line) alkoxyamine in the presence of HNE (0.68 μM). Signals without HNE are blue line for 75 μM, yellow line for 150 μM, and orange line for 250 μM of alkoxyamine. Doxorubicin treatment is a positive control of apoptosis (black columns). The negative control, HNE treatment without alkoxyamine, is represented by gray columns. The viability control which is only cells is represented by white columns.

main substrate selection is done at the P′1 position, the alkoxyamine should be modified to mimic the MMP preferred amino-acid at this position which is often a leucine. Again, docking experiments show that it is compatible with enzyme cleavage (not shown). As for cell permeability refinement for the alkyl radical, the modular nature of our model should allow these modifications. Our models may also be modified for osidase activities by replacing the peptide by a specific glycoside motif. Hence, heparanase, beta-glycosidase, or beta-galactosidase often reported as overexpressed in the tumor microenvironment[46,47] could be efficiently targeted.

■ MATERIAL AND METHODS

Synthesis. *Experimental Section.* Solvents and reactants for the preparation of alkoxyamines were used as received. Routine reaction monitoring was performed using silica gel 60 F254 TLC plates; spots were visualized upon exposure to UV light and a phosphomolybdic acid solution in EtOH, followed by heating. Purifications were performed on Reveleris X2 Flash System BUCHI switzerland. Cartouches flash Reveleris and GraceResolv: silica 40 μm. ^{1}H and ^{13}C NMR spectra were recorded in CDCl$_3$, CD$_3$OD, DMSO-d_6 on a 300 or 400 MHz spectrometer. Chemical shifts (δ) in ppm were reported using residual

nondeuterated solvents as internal references for ^{1}H and ^{13}C NMR spectra. High-resolution mass spectra (HRMS) were obtained on a SYNAPT G2 HDMS (Waters) spectrometer equipped with a pneumatically assisted atmospheric pressure ionization source. Positive mode electrospray ionization was used on samples: electrospray voltage: 2800 V; opening voltage: 20 V; nebulizer gas pressure (nitrogen): 800 L/h. Low resolution mass spectra were recorded on the ion trap AB SCIEX 3200 QTRAP equipped with an electrospray source. The parent ion $[M + H]^+$ is quoted.

Purity of final compounds was >95% as assessed by NMR spectra for all compounds and by HPLC for compound **1a**.

4-Vinylphenyl-(tert-butoxycarbonyl)valinamide (6). To a stirred solution of 4-vinylaniline **5** (1.0 g, 1 equiv, 8.37 mmol) and Boc-Val-OH (2.0 g, 1.1 equiv, 9.20 mmol) was added 1-hydroxybenzotriazole hydrate (HOBt, 1.24 g, 1.1 equiv, 9.20 mmol). After 15 min, the solution was cooled to 0 °C, and dicyclohexylcarbodiimide (DCC, 1.90 g, 1.1 equiv, 9.20 mmol) was added. The solution was stirred overnight at room temperature. The resulting suspension was filtered, and the organic phase was washed with HCl 1 M, NaHCO$_3$ sat., and brine and dried over MgSO$_4$. After concentration under reduced pressure, the residue was purified by column chromatography (DCM/MeOH 98:2) to afford the compound **6** (2.1 g, 78%). ^{1}H NMR (400 MHz, CDCl$_3$): δ 8.99 (s, 1H), 7.42 (d, J = 8.1 Hz, 2H), 7.20 (d, J = 8.2 Hz, 2H), 6.60 (dd, J = 17.6, 10.9 Hz, 1H), 5.64 (m, 2H), 5.15 (d, J = 10.9 Hz, 1H), 4.20 (m, 1H), 2.16 (m, 1H), 1.42 (s, 9H), 1.03 (m, 6H). ^{13}C NMR (101 MHz, CDCl$_3$): δ 171.0 (C), 156.7 (C), 137.5 (C), 136.3 (CH), 133.7 (C), 126.7 (2 × CH aro), 120.1 (2 × CH aro), 112.9 (CH$_2$), 80.3 (C), 61.2 (CH), 31.2 (CH), 28.5 (3 × CH$_3$), 19.5 (CH$_3$), 18.6 (CH$_3$). HRMS m/z (ESI): calcd for C$_{18}$H$_{27}$N$_2$O$_3{}^+$ $[M + H]^+$, 319.2016; found, 319.2020.

General Procedure for Coupling using Salen/Mn for the Preparation of 1b and 2b. To a stirred solution of Salen ligand (0.15 equiv) in *i*-PrOH was added MnCl$_2$ (0.15 equiv) in an open flask. After 30 min of stirring at room temperature, a solution of nitroxide (1 equiv) and 4-vinylphenyl-(*tert*-butoxycarbonyl)valinamide **6** (1.1 equiv) in *i*-PrOH was added first, and then solid NaBH$_4$ (4 equiv) was added in small portions. The resulting suspension was stirred at room temperature for 7 h. It was then diluted with EtOAc (100 mL), and 1 M aq HCl was carefully added. Solid NaHCO$_3$ was then added until neutralization. The layers were separated, and the organic phase was washed with water and brine and dried over MgSO$_4$. After concentration under reduced pressure, the residue was purified by column chromatography (petroleum ether/EtOAc) to afford the corresponding alkoxyamines **1b** and **2b**.

4-(1-((2,2,6,6-Tetramethylpiperidin-1-yl)oxy)ethyl)phenyl-(tert-butoxycarbonyl)valinamide (1b). Alkoxyamine **1b** was prepared according to the general procedure using Salen ligand (515 mg, 1.92 mmol), MnCl$_2$ (379 mg, 1.92 mmol), TEMPO (2.0 g, 12.80 mmol), 4-vinylphenyl-(*tert*-butoxycarbonyl)valinamide (4.5 g, 14.08 mmol), and NaBH$_4$ (1.9 g, 51.20 mmol). Alkoxyamine was purified by automatic flash column chromatography (petroleum ether/EtOAc; gradient: 100 to 80%) to afford **1b** (3.96 g, 65%). ^{1}H NMR (400 MHz, CDCl$_3$): δ 8.54 (s, 1H), 7.44 (d, J = 8.5 Hz, 2H), 7.20 (d, J = 8.1 Hz, 2H), 5.49 (dd, J = 9.0, 2.4 Hz, 1H), 4.72 (q, J = 6.6 Hz, 1H), 4.11 (m, 1H), 2.19 (m, 1H), 1.43 (m, J = 5.9 Hz, 16H), 1.26 (m, 3H), 1.14 (m, 3H), 1.01 (m, 9H), 0.65 (s, 3H). ^{13}C NMR (75 MHz, CDCl$_3$): δ 170.8 (C), 156.5 (C), 141.7 (C), 136.5 (C), 127.0 (2 × CH aro), 119.8 (2 × CH aro), 82.7 (CH), 79.9 (C), 61.0 (CH), 59.6 (2 × C), 40.3 (2 × CH$_2$), 34.3 (CH$_3$), 31.1 (CH), 28.4 (3 × CH$_3$), 23.5 (CH$_3$), 20.3 (2 × CH$_3$), 19.4 (CH$_3$), 18.5 (CH$_3$), 17.2 (CH$_2$). HRMS m/z (ESI): calcd for C$_{27}$H$_{46}$N$_3$O$_4{}^+$ $[M + H]^+$, 476.3483; found, 476.3478.

4-(1-((Di-tert-Butylamino)oxy)ethyl)phenyl)-(tert-butoxycarbonyl)valinamide (2b). Alkoxyamine **2b** was prepared according to the general procedure using Salen ligand (276 mg, 1.03 mmol), MnCl$_2$ (204 mg, 1.03 mmol), DBNO (1.0 g, 6.88 mmol), 4-vinylphenyl-(*tert*-butoxycarbonyl)valinate (2.4 g, 7.57 mmol), and NaBH$_4$ (1.1 g, 27.60 mmol). Alkoxyamine was purified by automatic flash column chromatography (petroleum ether/EtOAc; gradient: 100 to 80%) to afford **2b** (1.86 g, 57%). ^{1}H NMR (300 MHz, CDCl$_3$): δ 8.80 (s, 1H), 7.27 (d, J = 8.1 Hz, 2H), 6.99 (d, J = 7.9 Hz, 2H), 5.59 (d, J = 8.7 Hz, 1H), 4.57 (q, J = 6.6 Hz, 1H), 4.00 (m, 1H), 1.99 (m, 1H),

1.23 (m, 12H), 1.10 (s, 9H), 0.85 (m, 15H). ^{13}C NMR (75 MHz, CDCl$_3$): δ 170.9 (C), 156.5 (C), 141.2 (C), 136.6 (C), 127.3 (2 × CH aro), 119.8 (2 × CH aro), 82.4 (CH), 79.9 (C), 61.9 (C), 61.7 (C), 61.0 (CH), 31.1 (CH), 30.7 (6 × CH$_3$), 28.4 (3 × CH$_3$), 22.6 (CH$_3$), 19.4 (CH$_3$), 18.5 (CH$_3$). HRMS m/z (ESI): calcd for C$_{26}$H$_{46}$N$_3$O$_4^+$ [M + H]$^+$, 464.3483; found, 464.3488.

4-Acetylphenyl (tert-Butoxycarbonyl)valinate (8). To a stirred solution of 4-hydroxyacetophenone **7** (10 g, 2 equiv, 73.44 mmol) and Boc-Val-OH (8 g, 1 equiv, 36.72 mmol) in DCM (100 mL) were added successively DMAP (2.2 g, 0.5 equiv, 18.36 mmol) and DCC (11.4 g, 1.5 equiv, 55.08 mmol). The solution was stirred at room temperature overnight. Then, the resulting suspension was filtered, and the organic phase was washed with HCl 1 M (75 mL), NaHCO$_3$ sat. (75 mL), and brine (50 mL) and dried over MgSO$_4$. After concentration under reduced pressure, the residue was purified by column chromatography (DCM/MeOH 98:2) to afford the compound **8** (12.1 g, 98%). ^{1}H NMR (300 MHz, CDCl$_3$): δ 7.98 (d, J = 8.7 Hz, 2H), 7.19 (d, J = 8.7 Hz, 2H), 5.08 (d, J = 9.0 Hz, 1H, NH), 4.45 (dd, J = 9.1, 4.9 Hz, 1H), 2.58 (s, 3H), 2.32 (m, 1H), 1.46 (s, 9H), 1.08 (d, J = 6.9 Hz, 3H), 1.02 (d, J = 6.9 Hz, 3H). ^{13}C NMR (75 MHz, CDCl$_3$): δ 196.7 (C), 170.6 (C), 155.7 (C), 154.1 (C), 134.9 (C), 129.9 (2 × CH aro), 121.6 (2 × CH aro), 80.1 (C), 58.8 (CH), 31.2 (CH), 28.2 (3 × CH$_3$), 26.5 (CH$_3$), 19.1(CH$_3$), 17.7 (CH$_3$). HRMS m/z (ESI): calcd for C$_{18}$H$_{26}$NO$_5^+$ [M + H]$^+$, 336.1805; found, 336.1803.

4-(1-Hydroxyethyl)phenyl (tert-Butoxycarbonyl)valinate (9). To a stirred solution of **8** (2 g, 1 equiv, 5.96 mmol) in THF/MeOH (2:1) at 0 °C was added NaBH$_4$ (338 mg, 1.5 equiv, 8.943 mmol). The solution was stirred at 0 °C for 15 min. After this time, water was added and solvents were evaporated. The resulting aqueous solution was extracted with DCM, and the organic phase was washed brine and dried over MgSO$_4$. After concentration under reduced pressure, the residue was purified by column chromatography (DCM/MeOH 98:2) to afford the compound **9** (1.15 g, 57%). ^{1}H NMR (400 MHz, CDCl$_3$): δ 7.37 (d, J = 8.6 Hz, 2H), 7.05 (d, J = 8.6 Hz, 2H), 5.10 (d, J = 9.0 Hz, 1H, NH), 4.88 (q, J = 6.4 Hz, 1H), 4.43 (dd, J = 9.2, 4.8 Hz, 1H), 2.31 (m, 1H), 1.46 (m, 12H), 1.07 (d, J = 6.8 Hz, 3H), 1.01 (d, J = 6.9 Hz, 3H). ^{13}C NMR (101 MHz, CDCl$_3$): δ 171.1 (C), 155.7 (C), 149.6 (C), 143.8 (C), 126.6 (2 × CH aro), 121.3 (2 × CH aro), 80.0 (C), 69.8 (CH), 58.7 (CH), 31.4 (CH), 28.3 (3 × CH$_3$), 25.2 (CH$_3$), 19.1 (CH$_3$), 17.7 (CH$_3$). HRMS m/z (ESI): calcd for C$_{18}$H$_{28}$NO$_5^+$ [M + H]$^+$, 338.1962; found, 338.1959.

4-(1-bromoethyl)phenyl (tert-butoxycarbonyl)valinate (10). To a stirred solution of **9** (2 g, 1 equiv, 5.96 mmol) in DCM at 0 °C were added CBr$_4$ (2.95 g, 1.5 equiv, 8.89 mmol) and triphenylphosphine (2.33 g, 1.5 equiv, 8.89 mmol). The solution was stirred at 0 °C for 15 min and room temperature for 1 h. After this time, DCM was evaporated under reduced pressure and the residue was purified by column chromatography (DCM/MeOH 98:2) to afford the compound **10** (2.2 g, 92%). ^{1}H NMR (400 MHz, CDCl$_3$): δ 7.44 (d, J = 8.6 Hz, 2H), 7.07 (d, J = 8.6 Hz, 2H), 5.19 (q, J = 6.9 Hz, 1H), 5.07 (d, J = 9.0 Hz, 1H, NH), 4.44 (dd, J = 9.2, 4.9 Hz, 1H), 2.31 (m, 1H), 2.02 (d, J = 6.9 Hz, 3H), 1.46 (s, 9H), 1.07 (d, J = 6.8 Hz, 3H), 1.01 (d, J = 6.9 Hz, 3H). ^{13}C NMR (101 MHz, CDCl$_3$): δ 170.9 (C), 155.7 (C), 150.1 (C), 141.0 (C), 128.0 (2 × CH aro), 121.5 (2 × CH aro), 80.0 (C), 58.7 (CH), 48.3 (CH), 31.3 (CH), 28.3 (3 × CH$_3$), 26.8 (CH$_3$), 19.0 (CH$_3$), 17.7 (CH$_3$). HRMS m/z (ESI): calcd for C$_{18}$H$_{30}$N$_2$O$_4$Br$^+$ [M + H]$^+$, 419.1365; found, 419.1365.

General Procedure for ATRA Coupling for Preparation of 3b and 4b. To a degassed solution of CuBr (0.55 equiv) and Cu (1.1 equiv) in benzene, N,N,N',N'',N''-Pentamethyldiethylenetriamine (PMDETA, 0.55 equiv) was added dropwise, and the solution was kept under argon bubbling for another 30 min. Then, a degassed benzene solution of nitroxide (1 equiv) and **10** (1.1 equiv) was added, and the mixture was stirred for 3 h at room temperature under argon. Then, Et$_2$O, water, and NH$_4$OH were added and the mixture was washed with Et$_2$O. The organic layer was washed with H$_2$O and brine, dried with MgSO$_4$, and the solvent was evaporated to yield a crude product. The compound was purified by flash column chromatography (petroleum ether/EtOAc) to afford the corresponding alkoxyamines **3b** and **4b**.

4-(1-((2,2,6,6-tetramethylpiperidin-1-yl)oxy)ethyl)phenyl (tert-butoxycarbonyl)valinate (3b). Alkoxyamine **3b** was prepared according to the ATRA general procedure using CuBr (1.02 g, 7.04 mmol), Cu (888 mg, 14.08 mmol), PMDETA (1.47 mL, 7.04 mmol), TEMPO (2 g, 12.80 mmol), and 4-(1-bromoethyl)phenyl (t-butoxycarbonyl)valinate (5.6 g, 14.08 mmol). Alkoxyamine was purified by automatic flash column chromatography (petroleum ether/EtOAc; gradient: 100% to 70%) to afford **3b** (5.2 g, 86%). ^{1}H NMR (400 MHz, CDCl$_3$): δ 7.29 (d, J = 8.5 Hz, 2H), 7.00 (d, J = 8.5 Hz, 2H), 5.16 (d, J = 9.1 Hz, 1H), 4.76 (q, J = 6.6 Hz, 1H), 4.43 (dd, J = 9.1, 4.8 Hz, 1H), 2.34 (m, 1H), 1.52 (m, 16H), 1.36 (m, 2H), 1.26 (s, 3H), 1.13 (s, 3H), 1.05 (d, J = 6.8 Hz, 3H), 0.99 (m, 6H), 0.64 (s, 3H). ^{13}C NMR (101 MHz, CDCl$_3$): δ 170.8 (C), 155.4 (C), 149.0 (C), 143.3 (C), 127.4 (2 × CH aro), 120.6 (2 × CH aro), 82.2 (CH), 79.6 (C), 59.4 (2 × C), 58.5 (CH), 40.1 (2 × CH$_2$), 34.2 (CH$_3$), 34.0 (CH$_3$), 31.1 (CH), 28.1 (3 × CH$_3$), 23.1 (CH$_3$), 20.1 (2 × CH$_3$), 18.8 (CH$_3$), 17.5 (CH$_3$), 16.9 (CH$_2$). HRMS m/z (ESI): calcd for C$_{27}$H$_{45}$N$_2$O$_5^+$ [M + H]$^+$, 477.3323; ound, 477.3324.

4-(1-((di-tert-butylamino)oxy)ethyl)phenyl (tert-butoxycarbonyl)valinate (4b). Alkoxyamine **4b** was prepared according to the ATRA general procedure using CuBr (490 mg, 3.37 mmol), Cu (425 mg, 6.74 mmol), PMDETA (0.705 mL, 3.37 mmol), DBNO (890 g, 6.13 mmol), and 4-(1-bromoethyl)phenyl (t-butoxycarbonyl)valinate (2.7 g, 6.74 mmol). Alkoxyamine was purified by automatic flash column chromatography (petroleum ether/EtOAc; gradient: 100% to 70%) to afford **4b** (2.6 g, 93%). ^{1}H NMR (300 MHz, CDCl$_3$): δ 7.54 (d, J = 8.5 Hz, 2H), 7.25 (d, J = 8.5 Hz, 2H), 5.37 (d, J = 9.1 Hz, 1H), 5.05 (q, J = 6.7 Hz, 1H), 4.68 (m, 1H), 2.54 (m, 1H), 1.70 (m, 12H), 1.52 (s, 9H), 1.28 (m, 15H). ^{13}C NMR (75 MHz, CDCl$_3$): δ 171.1 (C), 155.7 (C), 149.3 (C), 143.1 (C), 128.0 (2 × CH aro), 120.8 (2 × CH aro), 82.1 (CH), 79.8 (C), 61.9 (C), 61.8 (C), 58.7 (CH), 31.4 (CH), 30.7 (6 × CH$_3$), 28.3 (3 × CH$_3$), 22.6 (CH$_3$), 19.1 (CH$_3$), 17.7 (CH$_3$). HRMS m/z (ESI): calcd for C$_{26}$H$_{45}$N$_2$O$_5^+$ [M + H]$^+$, 465.3323; found, 465.3320.

General Procedure for Boc-Ala-Ala-Pro-OH Coupling for the Preparation of 1c-4c. To a stirred solution of NHBoc-alkoxyamines **1b−4b** (1 equiv) in DCM was added trifluoroacetic acid (10 eq). After 2 h at room temperature, toluene was added and the solvents were evaporated. The addition of toluene and the coevaporation of the TFA is repeated three times and the resulting deprotected alkoxyamines was used in the next step without any more purification.

To a stirred solution of TFA salt alkoxyamines in DCM was added DIPEA (1.1 equiv), and after 5 min, Boc-Ala-Ala-Pro-OH (1.1 equiv) and HOBt (1.1 equiv) were successively added. The reaction was stirred at 0 °C for 15 min, and then DCC (1.1 equiv) was added. After 5 min at 0 °C, the reaction was left overnight at room temperature. After this time, the resulting suspension was filtered and the organic phase was washed with HCl 1 M, NaHCO$_3$ sat., and brine and dried over MgSO$_4$. After concentration under reduced pressure, the residue was purified by column chromatography (DCM/MeOH) to afford alkoxyamines **1c−4c**.

4-(1-((2,2,6,6-tetramethylpiperidin-1-yl)oxy)ethyl)phenyl (tert-butoxycarbonyl)alanylalanylprolylvalinamide (1c). Alkoxyamines **1c** was prepared according to the general procedure using **1b** (5.0 g, 10.51 mmol), TFA (8.0 mL, 105.11 mmol), DIPEA (1.97 mL, 11.56 mmol), Boc-Ala-Ala-Pro-OH (4.13 g, 11.56 mmol), HOBt (1.56 g, 11.56 mmol), and DCC (2.38 g, 11.56 mmol). Alkoxyamine was purified by automatic flash column chromatography (DCM/MeOH 97:3) to afford **1c** (3.8 g, 51%). ^{1}H NMR (400 MHz, CDCl$_3$): δ 9.00 (s, 1H), 7.68 (s, 1H), 7.60 (d, J = 8.5 Hz, 1H), 7.44 (d, J = 8.3 Hz, 2H), 7.16 (d, J = 8.3 Hz, 2H), 5.42 (d, J = 8.0 Hz, 1H), 4.70 (m, 3H), 4.40 (m, 2H), 3.66 (m, 1H), 3.56 (m, 1H), 2.01 (m, 5H), 1.39 (m, 16H), 1.23 (m, 9H), 1.10 (s, 3H), 0.93 (m, 9H), 0.61 (s, 3H). ^{13}C NMR (101 MHz CDCl$_3$): δ 172.4 (C), 172.0 (C), 171.9 (C), 169.7 (C), 155.5 (C), 141.8 (C), 136.6 (C), 126.9 (2 × CH aro), 119.7 (2 × CH aro), 82.6 (CH), 79.9 (C), 59.8 (CH), 59.6 (2 × C), 59.5 (CH), 49.7 (CH), 47.4 (CH$_2$), 46.6 (CH), 40.3 (2 × CH$_2$), 34.4 (2 × CH$_3$), 30.8 (CH), 28.4 (CH$_2$), 28.3 (3 × CH$_3$), 25.1 (CH$_2$), 23.5 (CH$_3$), 20.3 (2 × CH$_3$), 19.4 (CH$_3$), 19.3 (CH$_3$), 18.4 (CH$_3$), 18.1 (CH$_3$), 17.2 (CH$_2$). HRMS m/z (ESI): calcd for C$_{38}$H$_{63}$N$_6$O$_7^+$ [M + H]$^+$, 715.4753; found, 715.4756.

4-(1-((di-tert-butylamino)oxy)ethyl)phenyl (tert-butoxycarbonyl)alanylalanylprolylvalinamide (2c). Alkoxyamine **2c** was prepared according to the general procedure using **2b** (2.6 g, 6.03 mmol), TFA (4.6 mL, 60.31 mmol), DIPEA (1.13 mL, 6.63 mmol), Boc-Ala-Ala-Pro-OH (2.37 g, 6.63 mmol), HOBt (895 mg, 6.63 mmol), and DCC (1.37 g, 6.63 mmol). Alkoxyamine was purified by automatic flash column chromatography (DCM/MeOH 97:3) to afford **2c** (2.4 g, 58%). ^{1}H NMR (400 MHz, CDCl$_3$): δ 8.73 (d, J = 4.7 Hz, 1H), 7.48 (m, 4H), 7.22 (d, J = 8.5 Hz, 2H), 5.31 (d, J = 7.8 Hz, 1H), 4.74 (m, 3H), 4.40 (m, 2H), 3.71 (m, 1H), 3.59 (dt, J = 7.4, 5.0 Hz, 1H), 2.13 (m, 5H), 1.44 (m, 12H), 1.29 (m, 15H), 1.02 (s, 9H), 0.96 (d, J = 6.7 Hz, 3H), 0.92 (d, J = 6.7 Hz, 3H). ^{13}C NMR (101 MHz, CDCl$_3$): δ 172.3 (C), 172.2 (C), 171.8 (C), 169.5 (C), 155.4 (C), 141.4 (C), 136.6 (C), 127.4 (2 × CH aro), 119.7 (2 × CH aro), 82.4 (CH), 80.0 (C), 61.9 (C), 61.7 (C), 60.0 (CH), 59.5 (CH), 49.8 (CH), 47.5 (CH$_2$), 46.7 (CH), 30.7 (6 × CH$_3$), 28.4 (3 × CH$_3$) 28.3 (CH$_2$), 25.1 (CH$_2$), 22.6 (CH$_3$), 19.4 (CH$_3$), 19.1 (CH$_3$), 18.2 (CH$_3$), 18.1 (CH$_3$). HRMS m/z (ESI): calcd for C$_{37}$H$_{63}$N$_6$O$_7^+$ [M + H]$^+$, 703.4753; found: 703.4755.

4-(1-((2,2,6,6-tetramethylpiperidin-1-yl)oxy)ethyl)phenyl (tert-butoxycarbonyl)alanylalanylprolylvalinate (3c). Alkoxyamine **3c** was prepared according to the general procedure using **3b** (900 mg, 1.89 mmol), TFA (1.4 mL, 18.89 mmol), DIPEA (0.36 mL, 2.08 mmol), Boc-Ala-Ala-Pro-OH (743 mg, 2.08 mmol), HOBt (281 mg, 2.08 mmol), and DCC (429 mg, 2.08 mmol). Alkoxyamine was purified by automatic flash column chromatography (DCM/MeOH 97:3) to afford **3c** (980 mg, 73%). ^{1}H NMR (400 MHz, CDCl$_3$): δ 7.44 (m, 2H, 2 × NH), 7.29 (d, J = 8.5 Hz, 2H), 7.00 (d, J = 8.5 Hz, 2H), 5.16 (d, J = 7.3 Hz, 1H), 4.77 (m, 2H), 4.69 (m, 2H), 4.32 (m, 1H), 3.69 (m, 1H), 3.60 (m, 1H), 2.32 (m, 2H), 2.16 (m, 1H), 1.99 (m, 2H), 1.44 (m, 16H), 1.34 (m, 5H), 1.26 (m, 6H), 1.14 (s, 3H), 1.00 (m, 9H), 0.64 (s, 3H). ^{13}C NMR (101 MHz,, CDCl$_3$): δ 172.1 (C), 171.9 (C), 171.1 (C), 170.3 (C), 155.3 (C), 149.1 (C), 143.5 (C), 127.54 (2 × CH aro), 120.74 (2 × CH aro), 82.4 (CH), 79.9 (C), 59.7 (2 × C), 59.6 (CH), 57.4 (CH), 49.8 (CH), 47.3 (CH$_2$), 46.5 (CH), 40.3 (2 × CH$_2$), 34.2 (2 × CH$_3$), 31.0 (CH), 28.3 (3 × CH$_3$), 27.4 (CH$_2$), 25.0 (CH$_2$), 23.4 (CH$_3$), 20.3 (2 × CH$_3$), 19.1 (2 × CH$_3$), 18.4 (CH$_3$), 17.7 (CH$_3$), 17.1 (CH$_2$). HRMS m/z (ESI): calcd for C$_{38}$H$_{62}$N$_5$O$_8^+$ [M + H]$^+$, 716.4593; found, 716.4594.

4-(1-((di-tert-butylamino)oxy)ethyl)phenyl (tert-butoxycarbonyl)alanylalanylprolylvalinate (4c). Alkoxyamine **4c** was prepared according to the general procedure using **4b** (2.2 g, 4.74 mmol), TFA (3.6 mL, 47.44 mmol), DIPEA (0.89 mL, 5.21 mmol), Boc-Ala-Ala-Pro-OH (1.86 g, 5.21 mmol), HOBt (704 mg, 5.21 mmol), and DCC (1.07 g, 5.21 mmol). Alkoxyamine was purified by automatic flash column chromatography (DCM/MeOH 97:3) to afford **4c** (1.9 g, 57%). ^{1}H NMR (400 MHz, CDCl$_3$): δ 7.60 (d, J = 7.9 Hz, 1H), 7.47 (d, J = 8.6 Hz, 1H), 7.29 (d, J = 8.5 Hz, 2H), 6.99 (d, J = 8.5 Hz, 2H), 5.25 (d, J = 8.1 Hz, 1H), 4.80 (m, 2H), 4.69 (m, 2H), 4.40 (d, J = 9.1 Hz, 1H), 3.65 (m, 2H), 2.30 (m, 2H), 2.15 (m, 1H), 1.99 (m, 2H), 1.45 (d, J = 3.9 Hz, 3H), 1.40 (s, 9H), 1.33 (d, J = 6.8 Hz, 3H), 1.25 (m, 12H), 0.99 (m, 15H). ^{13}C NMR (101 MHz, CDCl$_3$): δ 172.0 (2 × C), 171.4 (C), 170.4 (C), 155.4 (C), 149.3 (C), 143.0 (C), 127.9 (2 × CH aro), 120.8 (2 × CH aro), 82.1 (CH), 79.9 (C), 61.9 (C), 61.8 (C), 59.7 (CH), 57.4 (CH), 49.7 (CH), 47.4 (CH$_2$), 46.5 (CH), 31.0 (CH), 30.6 (6 × CH$_3$), 28.3 (3 × CH$_3$), 27.7 (CH$_2$), 25.1 (CH$_2$), 22.6 (CH$_3$), 19.5 (CH$_3$), 19.2 (CH$_3$), 18.5 (CH$_3$), 17.8 (CH$_3$). HRMS m/z (ESI): calcd for C$_{37}$H$_{62}$N$_5$O$_8^+$ [M + H]$^+$, 704.4593; found, 704.4595.

General Procedure for Succinyl Group Coupling for the Preparation of 1a-4a. To a stirred solution of NHBoc-alkoxyamines **1c−4c** (1 equiv) in DCM was added trifluoroacetic acid (10 eq). After 2 h at room temperature, toluene was added and the solvents were evaporated. The addition of toluene and the coevaporation of the TFA is repeated three times and the resulting deprotected alkoxyamines were used in the next step without any more purification.

To a stirred solution of TFA salt alkoxyamines in DCM was added DIPEA (1.1 equiv), and after 5 min, anhydride succinic (1.1 eq) was added. The reaction was stirred at room temperature for 2 h. After concentration under reduced pressure, the residue was purified by preparative column chromatography (H$_2$O/MeOH) to afford alkoxyamines **1a−4a**.

Acid 4-((1-((1-(2-((3-methyl-1-oxo-1-((4-(1-((2,2,6,6-tetramethyl-piperidin-1-yl)oxy)ethyl)phenyl)amino)butan-2-yl)carbamoyl)-pyrrolidin-1-yl)-1-oxopropan-2-yl)amino)-1-oxopropan-2-yl)-amino)-4-oxobutanoic (1a). Alkoxyamine **1a** was prepared according to the general procedure using **1c** (220 mg, 0.31 mmol), TFA (235 μL, 3.07 mmol), DIPEA (58 μL, 0.34 mmol), and anhydride succinic (34 mg, 0.34 mmol) Alkoxyamine was purified by automatic preparative chromatography (H$_2$O/MeOH) to afford **1a** (222 mg, 86%). ^{1}H NMR (300 MHz, CD$_3$OD): δ 7.52 (d, J = 8.5 Hz, 2H), 7.25 (d, J = 8.6 Hz, 2H), 4.76 (q, J = 6.6 Hz, 1H), 4.58 (m, 2H), 4.36 (q, J = 7.1 Hz, 1H), 4.28 (d, J = 7.2 Hz, 1H), 3.73 (m, 2H), 2. 52 (m, 4H), 2.07 (m, 5H), 1.45 (m, 6H), 1.35 (m, 12H), 1.17 (s, 3H), 1.02 (m, 9H), 0.64 (s, 3H). ^{13}C NMR (75 MHz, CD$_3$OD): δ 177.4 (C), 174.7 (2 × C), 174.3 (C), 173.4 (C), 171.9 (C), 142.9 (C), 138.2, (C) 128.1 (2 × CH aro), 121.0 (2 × CH aro), 84.0 (CH), 61.5 (CH), 60.9 (CH), 60.8 (2 × C), 55.7 (CH), 50.2 (CH), 48.6 (CH), 48.5 (CH$_2$), 41.4 (2 × CH$_2$), 34.8 (2 × CH$_3$), 32.3 (CH), 32.0 (CH$_2$), 31.3 (CH$_2$), 30.3 (CH$_2$), 26.0 (CH$_2$), 23.8 (CH$_3$), 20.8 (2 × CH$_3$), 19.8 (CH$_3$), 18.9 (CH$_3$), 18.1 (CH$_2$), 17.9 (CH$_3$), 17.0 (CH$_3$). HRMS m/z (ESI): calcd for C$_{37}$H$_{59}$N$_6$O$_8^+$ [M + H]$^+$, 715.4389; found: 715.4395.

Acid 4-((1-((1-(2-((1-((4-(1-((di-tert-butylamino)oxy)ethyl)-phenyl)amino)-3-methyl-1-oxobutan-2-yl)carbamoyl)pyrrolidin-1-yl)-1-oxopropan-2-yl)amino)-1-oxopropan-2-yl)amino)-4-oxobu-tanoic (2a). Alkoxyamine **2a** was prepared according to the general procedure using **2c** (1.6 g, 2.27 mmol), TFA (1.74 mL, 22.72 mmol), DIPEA (427 μL, 2.50 mmol), and anhydride succinic (250 mg, 2.50 mmol). Alkoxyamine was purified by automatic preparative chromatography (H$_2$O/MeOH) to afford **2a** (1.3 g, 81%). ^{1}H NMR (400 MHz, DMSO-d_6):δ 9.93 (s, 1H), 8.00 (m, 2H), 7.82 (d, J = 8.5 Hz, 1H), 7.54 (d, J = 8.5 Hz, 2H), 7.23 (d, J = 8.6 Hz, 2H), 4.74 (q, J = 6.6 Hz, 1H), 4.47 (m, 2H), 4.26 (m, 2H), 3.57 (m, 2H), 2.37 (m, 4H), 2.02 (m, 2H), 1.87 (m, 3H), 1.40 (d, J = 6.7 Hz, 3H), 1.26 (s, 9H), 1.20 (d, J = 6.8 Hz, 3H), 1.16 (d, J = 7.1 Hz, 3H), 0.99 (s, 9H), 0.90 (d, J = 6.7 Hz, 6H). ^{13}C NMR (101 MHz, DMSO-d_6): δ 173.8 (C), 171.8 (C), 171.3 (C), 170.8 (C), 170.7 (C), 169.8 (C), 139.6 (C), 137.6 (C), 127.1 (2 × CH aro), 118.9 (2 × CH aro), 81.6 (CH), 61.3 (C), 61.2 (C), 59.2 (CH), 58.5 (CH), 47.8 (CH), 46.6 (CH$_2$), 46.2 (CH), 30.7 (3 × CH$_3$), 30.4 (3 × CH$_3$), 30.3 (CH$_2$), 29.9 (CH), 29.2 (CH$_2$), 28.7 (CH$_2$), 24.5 (CH$_2$), 22.1 (CH$_3$), 19.2 (CH$_3$), 18.2 (CH$_3$), 18.1 (CH$_3$), 17.0 (CH$_3$). HRMS m/z (ESI): calcd for C$_{36}$H$_{59}$N$_6$O$_8^+$ [M + H]$^+$, 703.4389; found, 703.4391.

Acid 4-((1-((1-(2-((3-methyl-1-oxo-1-(4-(1-((2,2,6,6-tetramethyl-piperidin-1-yl)oxy)ethyl)phenoxy)butan-2-yl)carbamoyl)pyrrolidin-1-yl)-1-oxopropan-2-yl)amino)-1-oxopropan-2-yl)amino)-4-oxobu-tanoic (3a). Alkoxyamine **3a** was prepared according to the general procedure using **3c** (500 mg, 0.70 mmol), TFA (534 μL, 6.98 mmol), DIPEA (129 μL, 0.76 mmol), and anhydride succinic (77 mg, 0.76 mmol). Alkoxyamine was purified by automatic preparative chromatography (H$_2$O/MeOH) to afford **3a** (401 mg, 80%). ^{1}H NMR (400 MHz, CDCl$_3$): δ 8.21 (d, J = 8.2 Hz, 1H), 7.51 (d, J = 8.3 Hz, 1H), 7.29 (m, 3H), 7.00 (d, J = 8.4 Hz, 2H), 4.78 (m, 3H), 4.66 (m, 1H), 3.69 (m, 2H), 2.56 (m, 4H), 2.27 (m, 1H), 2.17 (m, 2H), 2.01 (m, 2H), 1.44 (m, 7H), 1.29 (m, 8H), 1.17 (m, 6H), 0.97 (m, 9H), 0.65 (s, 3H). ^{13}C NMR (101 MHz, CDCl$_3$): δ 175.6 (C), 172.6 (C), 172.2 (C), 171.9 (C), 171.9 (C), 170.6 (C), 149.3 (C), 143.7 (C), 127.7 (2 × CH aro), 120.9 (2 × CH aro), 82.5 (CH), 59.9 (2 × C), 59.6 (CH), 57.6 (CH), 48.7 (CH), 47.7 (CH$_2$), 46.6 (CH), 40.4 (2 × CH$_2$), 34.4 (2 × CH$_3$), 31.2 (CH$_2$), 31.1 (CH), 29.7 (CH$_2$), 28.6 (CH$_2$), 25.0 (CH$_2$), 23.5 (CH$_3$), 20.5 (2 × CH$_3$), 19.6 (CH$_3$), 19.2 (CH$_3$), 18.1 (CH$_3$), 17.9 (CH$_3$), 17.3 (CH$_2$). HRMS m/z (ESI): calcd for C$_{37}$H$_{58}$N$_5$O$_9^+$ [M + H]$^+$, 716.4229; found, 716.4230.

Acid 4-((1-((1-(2-((1-(4-(1-((di-tert-butylamino)oxy)ethyl)-phenoxy)-3-methyl-1-oxobutan-2-yl)carbamoyl)pyrrolidin-1-yl)-1-oxopropan-2-yl)amino)-1-oxopropan-2-yl)amino)-4-oxobutanoic Acid (4a). Alkoxyamine **4a** was prepared according to the general procedure using **4c** (500 mg, 0.71 mmol), TFA (544 μL, 7.10 mmol), DIPEA (133 μL, 0.78 mmol), and anhydride succinic (78 mg, 0.78 mmol). Alkoxyamine was purified by automatic preparative chromatography (H$_2$O/MeOH) to afford **4a** (380 mg, 76%). ^{1}H NMR (400

MHz, DMSO-d_6): δ 8.27 (d, J = 7.6 Hz, 1H), 7.98 (m, 2H), 7.36 (d, J = 8.5 Hz, 2H), 7.02 (d, J = 8.5 Hz, 2H), 4.82 (q, J = 6.6 Hz, 1H), 4.49 (m, 2H), 4.28 (m, 2H), 3.58 (m, 2H), 2.38 (m, 4H), 2.21 (m, 1H), 2.03 (m, 1H), 1.86 (m, 3H), 1.43 (d, J = 6.6 Hz, 3H), 1.27 (s, 9H), 1.19 (d, J = 6.9 Hz, 3H), 1.16 (d, J = 7.1 Hz, 3H), 1.02 (d, J = 4.7 Hz, 3H), 1.00 (s, 9H), 0.97 (d, J = 6.5 Hz, 3H). ^{13}C NMR (101 MHz, DMSO-d_6): δ 173.8 (C), 172.0 (C), 171.7 (C), 170.7 (C), 170.4 (C), 170.2 (C), 149.2 (C), 142.2 (C), 127.9 (2 × CH aro), 121.0 (2 × CH aro), 81.3 (CH), 61.4 (C), 61.3 (C), 58.8 (CH), 57.7 (CH), 47.8 (CH), 46.6 (CH$_2$), 46.1 (CH), 30.3 (6 × CH$_3$), 30.0 (CH$_2$), 29.8 (CH), 29.2 (CH$_2$), 28.8 (CH$_2$), 24.4 (CH$_2$), 22.1 (CH$_3$), 19.0 (CH$_3$), 18.3 (CH$_3$), 18.1 (CH$_3$), 16.9 (CH$_3$). HRMS m/z (ESI): calcd for C$_{36}$H$_{58}$N$_5$O$_9$$^+$ [M + H]$^+$, 704.4229; found, 704.4224.

Cell Culture. The U87 human glioblastoma cell line was purchased from ATCC (LGC standards, Molsheim, France). Cells were cultured in DMEM (Gibco corp.) supplemented with 10% fetal bovine serum (Gibco corporation) in humidified atmosphere with 5% CO$_2$ at 37 °C.

Measurements of Alkoxyamine Activation by HNE In Vitro. HNE was purchased from EPC Elastin Product Co. Inc. (Missouri, USA). The prodrugs were synthesized as previously described. The kinetic experiments were done in 50 mM HEPES buffer, 150 mM NaCl, 5 mM CaCl$_2$, 0.05% IGEPAL, pH 7.4. The activation of prodrugs was measured by detection of the stable nitroxides TEMPO or DBNO using an EMXnano EPR spectrometer (BRUKER, Germany). HNE (20 nM final) and the prodrugs (300 μM final) were loaded in capillaries, and acquisitions were performed at 37 °C with a temperature controller (BIO-I, NOXYGEN, Germany). Substrate and product concentrations were obtained using the Spincount module of Xenon software (BRUKER) and the EMXnano internal calibration.

Homolysis Rate Determination. Suc-AAPV-anilide-TEMPO 1 mM was reacted with or without 1.6 μM HNE in HEPES buffer 50 mM pH 7.4 and 150 mM NaCl for 1, 2, and 10 min at 37 °C. Reaction was stopped by adding the same volume of galvinoxyl in THF since THF denatures HNE. The shift of the alkoxyamine homolysis equilibrium by galvinoxyl was measured by monitoring TEMPO concentration with EPR.

Cell Treatment. The U87 cells were seeded and cultured during 48 h on 96 multi-well plates (CELLSTAR, Greiner Bio-One, Germany). Prior to prodrug deposition, the medium was exchanged to unsupplemented DMEM. To test the dose-dependent effect on viability, the prodrug in the range of 0−400 and 0.68 μM NE were then added in serum-free culture media. After 1 h of incubation, the cultured media was supplemented with 10% of serum and the cells were incubated during 24, 48, or 72 h. When needed, eglin C (10 μM) (CIBA-GEIGY), a NE inhibitor, and troxerutin (0 to 150 mM) (Santa Cruz Biotechnology), a free radical scavenger, were added in the cell culture media before HNE during the cell treatment protocol.

Viability Test. The PrestoBlue Cell Viability Reagent (Invitrogen) was used according to the manufacturer's instructions. The reagent is a resazurin-based solution, and the living cells convert resazurin to fluorescent resorufin. So, the amount of fluorescence is proportional to the number of living cells. Briefly, to realize this test, the cell viability reagent was warmed to room temperature and then 1/10th of the volume of cell viability reagent was added directly in culture media. After 30 min of incubation at 37 °C, the results were recorded using a Varioskan LUX multimode microplate reader (Thermo Scientific). Fluorescence was measured with an excitation wavelength of 560 nm and an emission wavelength of 590 nm.

Apoptosis and Necrosis Assay. RealTime-Glo Annexin V Apoptosis and Necrosis Assay (Promega) was used according to the manufacturer's instructions. The RealTime-Glo Annexin V Apoptosis and Necrosis Assay is a living cell assay that measures the exposure of phosphatidylserine on the cell surface during the apoptotic process and it includes a cell-impermeant profluorescent DNA dye to detect necrosis process. The annexin V binding is detected with a luminescence signal, and necrosis is detected with a fluorescence signal. To detail the protocol quickly, detection reagent was prepared and was added on the cell medium. After 60 min of incubation at 37 °C, the fluorescence (excitation: 485 nm and emission: 530 nm) was

recorded using a Varioskan LUX multimode microplate reader (Thermo Scientific).

Caspase 3/7 Assay. The Caspase-Glo 3/7 Assay (Promega) was used according to the manufacturer's instructions. The assay contains a luminogenic caspase 3/7 substrate in a reagent optimized for caspase and luciferase activity. Addition of the reagent on cell medium results in cell lysis followed by caspase cleavage of the substrate and then the action of luciferase to generate a luminescence signal which is proportional to the amount of caspase activity. The assay protocol was started by equilibrating of cell plate and caspase substrate at room temperature. Next the reagent was added in each well of plate, and the plate was incubated 15 min at room temperature. The luminescence was recorded using the Varioskan LUX multimode microplate reader (Thermo Scientific).

■ ASSOCIATED CONTENT

Ⓢ Supporting Information

The Supporting Information is available free of charge at https://pubs.acs.org/doi/10.1021/acs.jmedchem.2c00455.

> NMR spectrum (1H, 13C, and DEPT 135) and HRMS of alkoxyamines 1a-4a, 1b-4b, and 1c-4c and compounds 6 and 8−10 (PDF)

> Molecular formula strings (CSV)

■ AUTHOR INFORMATION

Corresponding Authors

Pierre Voisin − *Magnetic Resonance of Biological Systems, UMR 5536 CNRS-University of Bordeaux, Bordeaux 33076, France*; Email: pierre.voisin@rmsb.u-bordeaux.fr

Philippe Mellet − *Magnetic Resonance of Biological Systems, UMR 5536 CNRS-University of Bordeaux, Bordeaux 33076, France; INSERM, Bordeaux 33000, France;* ⊙ orcid.org/0000-0001-5499-9735; Email: philippe.mellet@rmsb.u-bordeaux.fr

Authors

Seda Seren − *Magnetic Resonance of Biological Systems, UMR 5536 CNRS-University of Bordeaux, Bordeaux 33076, France*

Jean-Patrick Joly − *Aix Marseille Univ, CNRS UMR 7273, ICR, Case 551, Marseille 13397, France*

Véronique Bouchaud − *Magnetic Resonance of Biological Systems, UMR 5536 CNRS-University of Bordeaux, Bordeaux 33076, France*

Gérard Audran − *Aix Marseille Univ, CNRS UMR 7273, ICR, Case 551, Marseille 13397, France*

Sylvain R. A. Marque − *Aix Marseille Univ, CNRS UMR 7273, ICR, Case 551, Marseille 13397, France;* ⊙ orcid.org/0000-0002-3050-8468

Complete contact information is available at:
https://pubs.acs.org/10.1021/acs.jmedchem.2c00455

Author Contributions

‖S.S. and J.-P.J. contributed equally.

Notes

The authors declare no competing financial interest.

■ ABBREVIATIONS

API, atmospheric pressure ionization source; EPR, electron paramagnetic resonance; HNE, human neutrophil elastase; HRMS, high-resolution mass spectra; MMP, matrix metalloproteinase; NE, neutrophil elastase

■ REFERENCES

(1) Sloane, B. F.; List, K.; Fingleton, B.; Matrisian, L. Proteases in Cancer: Significance for Invasion and Metastasis. In *Proteases: Structure and Function*; Brix, K., Stöcker, W., Eds.; Springer Vienna: Vienna, 2013; pp.491−550.

(2) Choi, K. Y.; Swierczewska, M.; Lee, S.; Chen, X. Protease-activated drug development. *Theranostics* **2012**, *2*, 156−179.

(3) Atkinson, J. M.; Siller, C. S.; Gill, J. H. Tumour endoproteases: the cutting edge of cancer drug delivery? *Br. J. Pharmacol.* **2008**, *153*, 1344−1352.

(4) Lerman, I.; Hammes, S. R. Neutrophil elastase in the tumor microenvironment. *Steroids* **2018**, *133*, 96−101.

(5) Xiong, S.; Dong, L.; Cheng, L. Neutrophils in cancer carcinogenesis and metastasis. *J. Hematol. Oncol.* **2021**, *14*, 173.

(6) Akizuki, M.; Fukutomi, T.; Takasugi, M.; Takahashi, S.; Sato, T.; Harao, M.; Mizumoto, T.; Yamashita, J.-i. Prognostic significance of immunoreactive neutrophil elastase in human breast cancer: long-term follow-up results in 313 patients. *Neoplasia* **2007**, *9*, 260−264.

(7) Sun, Z.; Yang, P. Role of imbalance between neutrophil elastase and alpha 1-antitrypsin in cancer development and progression. *Lancet Oncol.* **2004**, *5*, 182−190.

(8) Deryugina, E.; Carré, A.; Ardi, V.; Muramatsu, T.; Schmidt, J.; Pham, C.; Quigley, J. P. Neutrophil Elastase Facilitates Tumor Cell Intravasation and Early Metastatic Events. *iScience* **2020**, *23*, 101799.

(9) Xiao, Y.; Cong, M.; Li, J.; He, D.; Wu, Q.; Tian, P.; Wang, Y.; Yang, S.; Liang, C.; Liang, Y.; Wen, J.; Liu, Y.; Luo, W.; Lv, X.; He, Y.; Cheng, D.-d.; Zhou, T.; Zhao, W.; Zhang, P.; Zhang, X.; Xiao, Y.; Qian, Y.; Wang, H.; Gao, Q.; Yang, Q.-c.; Yang, Q.; Hu, G. Cathepsin C promotes breast cancer lung metastasis by modulating neutrophil infiltration and neutrophil extracellular trap formation. *Cancer Cell* **2021**, *39*, 423−437.

(10) Taya, M.; Garcia-Hernandez, M. d. l. L.; Rangel-Moreno, J.; Minor, B.; Gibbons, E.; Hammes, S. R. Neutrophil elastase from myeloid cells promotes TSC2-null tumor growth. *Endocr.-Relat. Cancer* **2020**, *27*, 261−274.

(11) Xiao, Z.; Hammes, S. R. AXL cooperates with EGFR to mediate neutrophil elastase-induced migration of prostate cancer cells. *iScience* **2021**, *24*, 103270.

(12) Yamashita, J.-I.; Ogawa, M.; Ikei, S.; Omachi, H.; Yamashita, S.-I.; Saishoji, T.; Nomura, K.; Sato, H. Production of immunoreactive polymorphonuclear leucocyte elastase in human breast cancer cells: possible role of polymorphonuclear leucocyte elastase in the progression of human breast cancer. *Br. J. Cancer* **1994**, *69*, 72−76.

(13) Lerman, I.; Garcia-Hernandez, M. d. l. L.; Rangel-Moreno, J.; Chiriboga, L.; Pan, C.; Nastiuk, K. L.; Krolewski, J. J.; Sen, A.; Hammes, S. R. Infiltrating Myeloid Cells Exert Protumorigenic Actions via Neutrophil Elastase. *Mol. Cancer Res.* **2017**, *15*, 1138−1152.

(14) Vaguliene, N.; Zemaitis, M.; Lavinskiene, S.; Miliauskas, S.; Sakalauskas, R. Local and systemic neutrophilic inflammation in patients with lung cancer and chronic obstructive pulmonary disease. *BMC Immunol.* **2013**, *14*, 36.

(15) Audran, G.; Brémond, P.; Franconi, J.-M.; Marque, S. R. A.; Massot, P.; Mellet, P.; Parzy, E.; Thiaudière, E. Alkoxyamines: a new family of pro-drugs against cancer. Concept for theranostics. *Org. Biomol. Chem.* **2014**, *12*, 719−723.

(16) Moncelet, D.; Voisin, P.; Koonjoo, N.; Bouchaud, V.; Massot, P.; Parzy, E.; Audran, G.; Franconi, J.-M.; Thiaudière, E.; Marque, S. R. A.; Brémond, P.; Mellet, P. Alkoxyamines: toward a new family of theranostic agents against cancer. *Mol. Pharm.* **2014**, *11*, 2412−2419.

(17) Audran, G.; Bosco, L.; Brémond, P.; Jugniot, N.; Marque, S. R. A.; Massot, P.; Mellet, P.; Moussounda Moussounda Koumba, T.; Parzy, E.; Rivot, A.; Thiaudière, E.; Voisin, P.; Wedl, C.; Yamasaki, T.

(18) Albalat, M.; Audran, G.; Holzritter, M.; Marque, S. R. A.; Mellet, P.; Vanthuyne, N.; Voisin, P. An enzymatic acetal/hemiacetal conversion for the physiological temperature activation of the alkoxyamine C−ON bond homolysis. *Org. Chem. Front.* **2020**, *7*, 2916−2924.

(19) Audran, G.; Marque, S. R. A.; Mellet, P. Smart Alkoxyamines: A New Tool for Smart Applications. *Acc. Chem. Res.* **2020**, *53*, 2828−2840.

(20) Dao, J.; Benoit, D.; Hawker, C. J. A versatile and efficient synthesis of alkoxyamine LFR initiators via manganese based asymmetric epoxidation catalysts. *J. Polym. Sci., Part A: Polym. Chem.* **1998**, *36*, 2161−2167.

(21) Neises, B.; Steglich, W. Simple Method for the Esterification of Carboxylic Acids. *Angew. Chem., Int. Ed. Engl.* **1978**, *17*, 522−524.

(22) Toda, N.; Tago, K.; Marumoto, S.; Takami, K.; Ori, M.; Yamada, N.; Koyama, K.; Naruto, S.; Abe, K.; Yamazaki, R.; Hara, T.; Aoyagi, A.; Abe, Y.; Kaneko, T.; Kogen, H. Design, synthesis and structure−Activity relationships of dual inhibitors of acetylcholinesterase and serotonin transporter as potential agents for Alzheimer's disease. *Bioorg. Med. Chem.* **2003**, *11*, 1935−1955.

(23) Harrisson, S.; Couvreur, P.; Nicolas, J. Simple and efficient copper metal-mediated synthesis of alkoxyamine initiators. *Polym. Chem.* **2011**, *2*, 1859−1865.

(24) Kothe, T.; Marque, S.; Martschke, R.; Popov, M.; Fischer, H. Radical reaction kinetics during homolysis of N-alkoxyamines: verification of the persistent radical effect. *J. Chem. Soc., Perkin Trans. 1* **1998**, *2*, 1553−1560.

(25) Huang, Y.; Lee, C.; Borgström, P.; Gjerset, R. A. Macrophage-mediated bystander effect triggered by tumor cell apoptosis. *Mol. Ther.* **2007**, *15*, 524−533.

(26) Alfano, R. W.; Leppla, S. H.; Liu, S.; Bugge, T. H.; Herlyn, M.; Smalley, K. S.; Bromberg-White, J. L.; Duesbery, N. S.; Frankel, A. E. Cytotoxicity of the matrix metalloproteinase-activated anthrax lethal toxin is dependent on gelatinase expression and B-RAF status in human melanoma cells. *Mol. Cancer Therapeut.* **2008**, *7*, 1218−1226.

(27) Shapiro, S. D.; Goldstein, N. M.; Houghton, A. M.; Kobayashi, D. K.; Kelley, D.; Belaaouaj, A. Neutrophil elastase contributes to cigarette smoke-induced emphysema in mice. *Am. J. Surg. Pathol.* **2003**, *163*, 2329−2335.

(28) Gregory, A. D.; Kliment, C. R.; Metz, H. E.; Kim, K.-H.; Kargl, J.; Agostini, B. A.; Crum, L. T.; Oczypok, E. A.; Oury, T. A.; Houghton, A. M. Neutrophil elastase promotes myofibroblast differentiation in lung fibrosis. *J. Leukoc. Biol.* **2015**, *98*, 143−152.

(29) Alfaidi, M.; Wilson, H.; Daigneault, M.; Burnett, A.; Ridger, V.; Chamberlain, J.; Francis, S. Neutrophil elastase promotes interleukin-1beta secretion from human coronary endothelium. *J. Biol. Chem.* **2015**, *290*, 24067−24078.

(30) Sato, T.; Takahashi, S.; Mizumoto, T.; Harao, M.; Akizuki, M.; Takasugi, M.; Fukutomi, T.; Yamashita, J.-i. Neutrophil elastase and cancer. *Surg. Oncol.* **2006**, *15*, 217−222.

(31) Dollery, C. M.; Owen, C. A.; Sukhova, G. K.; Krettek, A.; Shapiro, S. D.; Libby, P. Neutrophil elastase in human atherosclerotic plaques: production by macrophages. *Circulation* **2003**, *107*, 2829−2836.

(32) Vicuña, L.; Strochlic, D. E.; Latremoliere, A.; Bali, K. K.; Simonetti, M.; Husainie, D.; Prokosch, S.; Riva, P.; Griffin, R. S.; Njoo, C.; Gehrig, S.; Mall, M. A.; Arnold, B.; Devor, M.; Woolf, C. J.; Liberles, S. D.; Costigan, M.; Kuner, R. The serine protease inhibitor SerpinA3N attenuates neuropathic pain by inhibiting T cell-derived leukocyte elastase. *Nat. Med.* **2015**, *21*, 518−523.

(33) Kristensen, J. H.; Karsdal, M. A.; Sand, J. M.; Willumsen, N.; Diefenbach, C.; Svensson, B.; Hägglund, P.; Oersnes-Leeming, D. J. Serological assessment of neutrophil elastase activity on elastin during lung ECM remodeling. *BMC Pulm. Med.* **2015**, *15*, 53.

(34) Kistowski, M.; Dębski, J.; Karczmarski, J.; Paziewska, A.; Olędzki, J.; Mikula, M.; Ostrowski, J.; Dadlez, M. A Strong Neutrophil Elastase Proteolytic Fingerprint Marks the Carcinoma Tumor Proteome. *Mol. Cell. Proteomics* **2017**, *16*, 213−227.

(35) Houghton, A. M.; Rzymkiewicz, D. M.; Ji, H.; Gregory, A. D.; Egea, E. E.; Metz, H. E.; Stolz, D. B.; Land, S. R.; Marconcini, L. A.; Kliment, C. R.; Jenkins, K. M.; Beaulieu, K. A.; Mouded, M.; Frank, S. J.; Wong, K. K.; Shapiro, S. D. Neutrophil elastase-mediated degradation of IRS-1 accelerates lung tumor growth. *Nat. Med.* **2010**, *16*, 219−223.

(36) Starcher, B.; O'Neal, P.; Granstein, R. D.; Beissert, S. Inhibition of neutrophil elastase suppresses the development of skin tumors in hairless mice. *J. Invest. Dermatol.* **1996**, *107*, 159−163.

(37) Fan, S.; Xu, Y.; Li, X.; Tie, L.; Pan, Y.; Li, X. Opposite angiogenic outcome of curcumin against ischemia and Lewis lung cancer models: in silico, in vitro and in vivo studies. *Biochim. Biophys. Acta* **2014**, *1842*, 1742−1754.

(38) Xu, Y.; Zhang, J.; Han, J.; Pan, X.; Cao, Y.; Guo, H.; Pan, Y.; An, Y.; Li, X. Curcumin inhibits tumor proliferation induced by neutrophil elastase through the upregulation of alpha1-antitrypsin in lung cancer. *Mol. Oncol.* **2012**, *6*, 405−417.

(39) Ho, A.-S.; Chen, C.-H.; Cheng, C.-C.; Wang, C.-C.; Lin, H.-C.; Luo, T.-Y.; Lien, G.-S.; Chang, J. Neutrophil elastase as a diagnostic marker and therapeutic target in colorectal cancers. *Oncotarget* **2014**, *5*, 473−480.

(40) Inada, M.; Yamashita, J.; Ogawa, M. Neutrophil elastase inhibitor (ONO-5046-Na) inhibits the growth of human lung cancer cell lines transplanted into severe combined immunodeficiency (scid) mice. *Res. Commun. Mol. Pathol. Pharmacol.* **1997**, *97*, 229−232.

(41) Wada, Y.; Yoshida, K.; Hihara, J.; Konishi, K.; Tanabe, K.; Ukon, K.; Taomoto, J.; Suzuki, T.; Mizuiri, H. Sivelestat, a specific neutrophil elastase inhibitor, suppresses the growth of gastric carcinoma cells by preventing the release of transforming growth factor-alpha. *Cancer Sci.* **2006**, *97*, 1037−1043.

(42) Schechter, I.; Berger, A. On the size of the active site in proteases. I. Papain. *Biochem. Biophys. Res. Commun.* **1967**, *27*, 157−162.

(43) Busek, P.; Mateu, R.; Zubal, M.; Kotackova, L.; Sedo, A. Targeting fibroblast activation protein in cancer - Prospects and caveats. *Front. Biosci.* **2018**, *23*, 1933−1968.

(44) Hamson, E. J.; Keane, F. M.; Tholen, S.; Schilling, O.; Gorrell, M. D. Understanding fibroblast activation protein (FAP): substrates, activities, expression and targeting for cancer therapy. *Proteonomics Clin. Appl.* **2014**, *8*, 454−463.

(45) Santamaría, I.; Velasco, G.; Cazorla, M.; Fueyo, A.; Campo, E.; López-Otín, C. Cathepsin L2, a novel human cysteine proteinase produced by breast and colorectal carcinomas. *Cancer Res.* **1998**, *58*, 1624−1630.

(46) Rivara, S.; Milazzo, F. M.; Giannini, G. Heparanase: a rainbow pharmacological target associated to multiple pathologies including rare diseases. *Future Med. Chem.* **2016**, *8*, 647−680.

(47) Renoux, B.; Fangous, L.; Hötten, C.; Péraudeau, E.; Eddhif, B.; Poinot, P.; Clarhaut, J.; Papot, S. A beta-glucuronidase-responsive albumin-binding prodrug programmed for the double release of monomethyl auristatin E. *MedChemComm* **2018**, *9*, 2068−2071.